

Table 3 Single nucleotide polymorphisms (SNPs) on the disease chromosome of 16q22.1-linked autosomal dominant cerebellar ataxia (16q-ADCA). We identified thirteen SNPs by ourselves. SNP05 and SNP06 were absent in control chromosomes (n=200) and are thought to be highly specific to the disease chromosome

SNP/marker	Position on Chr 16	SNP change on 16q-ADCA	Frequency in control (%)
	GGAA05 64,938,933		
SNP01	64,972,150	A → G	27.8
SNP02	64,977,170	A → C	22.2
SNP03	64,977,733	T → C	30.0
SNP04	64,982,678	C → T	27.8
SNP05	65,049,292	G → A	0.0
	D16S397 65,295,770		
SNP06	65,337,827	A → G	0.0
SNP07	65,449,825	C → T	56.3
SNP08	65,451,833	T → A	45.5
	GGAA10 65,452,426		
SNP09	65,457,741	T → A	42.4
SNP10	65,458,302	T → C	45.5
SNP11	65,669,454	T → C	30.3
	GATA01 65,700,022		
SNP12	65,771,917	G → A	18.2
SNP13	65,793,152	C → T	8.7
<i>puratrophin-1</i> (C/T)	65,871,434	C → T	0.0

microsatellite markers. Within this region, we had found that the single nucleotide -16C>T substitution in the *puratrophin-1* gene was strongly associated with the disease (Ishikawa et al. 2005). Since then, a number of patients with the substitution and the common haplotype were reported in various areas of Japan. However, a report of the one exceptional patient without the substitution in the family in which all other affected subjects carried the substitution (Ohata et al. 2006) raised the possibility that a true pathogenic mutation may be present in a different gene. This exceptional patient indicated that the mutation might be lying centromeric to the substitution in the *puratrophin-1* gene, where the patient shared the common haplotype with other affected individuals in the family.

Here, we re-examined the 16q-ADCA families with the -16C>T substitution in the *puratrophin-1* gene with microsatellite markers and found four possible centromeric borders of the disease locus (GATA01, D16S397, GGAA10, GGAA05), based on the difference of alleles. We searched for informative SNPs around the markers capable of distinguishing the chromosomes derived from a founder and analyzed haplotypes with the SNPs. Because all of the examined families carried SNPs around the markers GATA01, D16S397, and GGAA10, ancestral chromosomal recombination around the markers was not confirmed. The differences in alleles for these markers was only one repeat-unit, suggesting that the allele differences

Table 4 The haplotype analysis with single nucleotide polymorphisms (SNPs). Fourteen families of 16q-ADCA with different alleles for microsatellite markers and family U09 are shown. The gray squares indicate that the family carried the SNPs common to 16q-ADCA. Family T46 did not carry the common SNPs from SNP01 to SNP04. This is consistent with the findings on microsatellite markers

(Table 1), further suggesting that the centromeric border of the disease locus is SNP04. Family U09 carried all of the 13 SNPs. This would also support the theory that family U09 shares the 16q-ADCA common haplotype centromeric to the substitution in the *puratrophin-1* gene

SNP	SNP change on 16q-ADCA	frequency in control (%)	family No.														U09
			P4	T3	T4	T5	T6	T7	T12	T15	T21	T28	T37	T43	T44	T46	
SNP01	A → G	27.8	G/A	G/A	G/A	G	G	G/A	G	G/A	G/A	G/A	G	G/A	G	A	G/A
SNP02	A → C	22.2	C/A	C/A	C/A	C	C	C/A	C	C/A	C/A	C/A	C	C/A	C/A	A	C/A
SNP03	T → C	30.0	C/T	C/T	C/T	C	C	C/T	C	C/T	C/T	C/T	C	C/T	C	T	C/T
SNP04	C → T	27.8	T/C	T	T/C	T	T	T/C	T	T/C	T/C	T	T	T/C	T	C	C/T
SNP05	G → A	0.0	A/G	A/G	A/G	A/G	A/G	A/G	A/G	A/G	A/G	A/G	A/G	A/G	A/G	A/G	A/G
SNP06	A → G	0.0	G/A	G/A	G/A	G/A	G/A	G/A	G/A	G/A	G/A	G/A	G/A	G/A	G/A	G/A	G/A
SNP07	C → T	56.3	T	T/C	T/C	T	T	T/C	T/C	T	T	T/C	T/C	T/C	T	T/C	T/C
SNP08	T → A	45.5	A	A/T	A/T	A	A	A/T	A/T	A	A	A/T	A/T	A/T	A	A/T	A
SNP09	T → A	42.4	A	A/T	A/T	A	A	A/T	A/T	A	A	A/T	A/T	A/T	A	A/T	A
SNP10	T → C	45.5	C	C/T	C/T	C	C	C/T	C/T	C	C	C/T	C/T	C/T	C/T	C/T	C/T
SNP11	T → C	30.3	C	C/T	C/T	C/T	C	C/T	C	C	C/T	C/T	C/T	C/T	C	C/T	C/T
SNP12	G → A	18.2	A	A/G	A/G	A/G	A/G	A/G	A/G	A	A/G	A/G	A/G	A/G	A	A/G	A/G
SNP13	C → T	8.7	T	C/T	C/T	C/T	C/T	C/T	C/T	C/T	C/T	C/T	C/T	C/T	T	C/T	C/T
<i>puratrophin-1</i> (C/T)	C → T	0.0	T	T	T	T	T/C	T/C	T/C	T/C	T/C	T/C	T/C	T/C	T/C	T/C	C

in GATA01, D16S397, and GGAA10 might have resulted not from recombination events, but from the microsatellite slippage mutation (Ikeda et al. 2004). On the other hand, four families (P4, T3, T25, T46) showed great allele differences in GGAA05 and one family (T46) did not carry four SNPs, confirming that family T46 did not share the genomic region centromeric to GGAA05 with the other 16q-ADCA families. This strongly indicates that the centromeric border of the disease locus of 16q-ADCA could be placed at SNP04.

The U09 family had the identical alleles for all markers and SNPs in the region centromeric to the $-16C>T$ substitution in the *puratrophin-1* gene. It is impossible to conclude that the family has the common haplotype of 16q-ADCA because only one examined family member was available for the present genetic analysis. However, carrying the rare alleles for GGAA05 and infrequent SNPs, both highly specific to the disease chromosome, strongly suggests that the U09 family shares a part of the 16q-ADCA common haplotype. The patient in the U09 family developed pure cerebellar ataxia later in life without apparent family history. Because 16q-ADCA patients were found among sporadic cases (Ouyang et al. 2006), these clinical features of the U09 family are consistent with those of 16q-ADCA. Importantly, this family had not been reported previously and, therefore, would be the second case of 16q-ADCA without the substitution in the *puratrophin-1* gene following the family reported by Ohata et al. (2006). These cases indicate that the telomeric end of the disease locus could be placed at the $-16C>T$ substitution in the *puratrophin-1* gene.

Haplotype analysis of a number of 16q-ADCA families with microsatellite markers and SNPs in this study suggests

that the gene locus of 16q-ADCA could be re-assigned to a 900-kb genomic region between SNP04 and the substitution in the *puratrophin-1* gene (Fig. 1). This region partly overlaps with, but is not the same as, the candidate region previously set by Ohata et al. (2006). They showed that three large 16q-ADCA families shared a common haplotype between D16S3086 and D16S412, and suggested the possibility that real pathogenic mutation would exist in the region between TTCC01 and the $-16C>T$ substitution in the *puratrophin-1* gene. However, the allele difference for TTCC01 in their families was only one repeat-unit, and all of their patients shared identical allele for TAGA02, lying centromeric to TTCC01. Since the possibility of slippage mutation remains as an explanation for the allele difference seen in TTCC01, as we observed for GATA01, D16S397, and GGAA10, it would be cautious to place the centromeric border at the marker TTCC01. Given that the allele differences in TTCC01 is due to slippage mutation, the centromeric border in their families would be alternatively set at D16S503, since an obligate recombination was seen between D16S503 and TAGA02. It would be, thus, important to analyze GGAA05 and specific SNPs in their families to see to what extent their patients harbor conserved haplotypes.

Although we found a patient without the $-16C>T$ substitution in the *puratrophin-1* gene, the substitution was present in all patients except the one in the U09 family (i.e., 125/126=99.2% sensitivity; 100% specificity) and, thus, the *puratrophin-1* genetic change still remains to be a useful marker. Molecular diagnosis with multiple microsatellite markers and SNPs will help to identify 16q-ADCA patients more accurately. Through the present study, we showed that the truly pathogenic mutation would lie in a 900-kb genomic region between SNP04 and the $-16C>T$ substitution in the *puratrophin-1* gene. Further investigations for finding a genetic mutation within the critical region are needed to elucidate the molecular pathogenesis of 16q-ADCA.

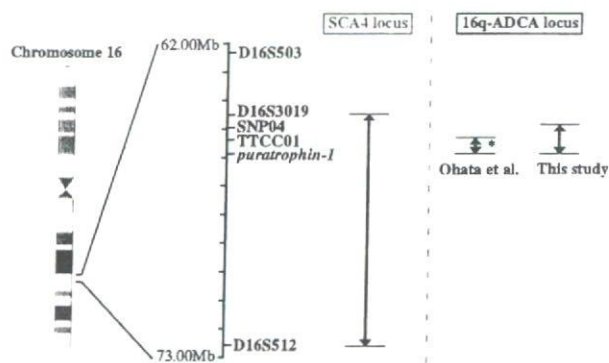


Fig. 1 A summary of critical intervals for 16q-ADCA and SCA4. Our study could define the disease locus of 16q-ADCA to a 900-kb genomic region between SNP04 and the $-16C>T$ substitution in the *puratrophin-1* gene. This region is completely inside the candidate locus of SCA4 (Flanigan et al. 1996). The haplotype region (asterisk) between TTCC01 and the *puratrophin-1* gene shown by Ohata et al. (2006) is also shown, together with an alternative critical region between D16S503 and the *puratrophin-1* gene (see text for details)

References

- Cagnoli C, Mariotti C, Taroni F, Seri M, Brussino A, Michielotto C, Grisoli M, Di Bella D, Migone N, Gellera C, Di Donato S, Brusco A (2006) SCA28, a novel form of autosomal dominant cerebellar ataxia on chromosome 18p11.22-q11.2. *Brain* 129:235–242
- Chen DH, Brkanac Z, Verlinde CL, Tan XJ, Bylenok L, Nochlin D, Matsushita M, Lipe H, Wolff J, Fernandez M, Cimino PJ, Bird TD, Raskind WH (2003) Missense mutations in the regulatory domain of PKC gamma: a new mechanism for dominant nonepisodic cerebellar ataxia. *Am J Hum Genet* 72:839–849
- Flanigan K, Gardner K, Alderson K, Galster B, Otterud B, Leppert MF, Kaplan C, Ptacek LJ (1996) Autosomal dominant spinocerebellar ataxia with sensory axonal neuropathy (SCA4): clinical description and genetic localization to chromosome 16q22.1. *Am J Hum Genet* 59:392–399

- Harding AE (1982) The clinical features and classification of the late onset autosomal dominant cerebellar ataxias. A study of 11 families, including descendants of the "Drew family of Walworth." *Brain* 105:1–28
- Hellenbroich Y, Pawlack H, Rub U, Schwinger E, Zuhlke Ch (2005) Spinocerebellar ataxia type 4. Investigation of 34 candidate genes. *J Neurol* 252:1472–1475
- Holmes SE, O'Hearn EE, McInnis MG, Gorelick-Feldman DA, Kleiderlein JJ, Callahan C, Kwak NG, Ingersoll-Ashworth RG, Sherr M, Sumner AJ, Sharp AH, Ananth U, Seltzer WK, Boss MA, Viera-Saecker A-M, Epplen JT, Riess O, Ross CA, Margolis RL (1999) Expansion of a novel CAG trinucleotide repeat in the 5' region of PPP2R2B is associated with SCA12. *Nat Genet* 23:391–392
- Ikeda Y, Dalton JC, Moseley ML, Gardner KL, Bird TD, Ashizawa T, Seltzer WK, Pandolfo M, Milunsky A, Potter NT, Shoji M, Vincent JB, Day JW, Ranum LP (2004) Spinocerebellar ataxia type 8: molecular genetic comparisons and haplotype analysis of 37 families with ataxia. *Am J Hum Genet* 75:3–16
- Ikeda Y, Dick KA, Weatherspoon MR, Gincel D, Armbrust KR, Dalton JC, Stevanin G, Durr A, Zuhlke C, Burk K, Clark HB, Brice A, Rothstein JD, Schut LJ, Day JW, Ranum LP (2006) Spectrin mutations cause spinocerebellar ataxia type 5. *Nat Genet* 38:184–190
- Ishikawa K, Tanaka H, Saito M, Ohkoshi N, Fujita T, Yoshizawa K, Ikeuchi T, Watanabe M, Hayashi A, Takiyama Y, Nishizawa M, Nakano I, Matsubayashi K, Miwa M, Shoji S, Kanazawa I, Tsuji S, Mizusawa H (1997) Japanese families with autosomal dominant pure cerebellar ataxia map to chromosome 19p13.1-p13.2 and are strongly associated with mild CAG expansions in the spinocerebellar ataxia type 6 gene in chromosome 19p13.1. *Am J Hum Genet* 61:336–346
- Ishikawa K, Toru S, Tsunemi T, Li M, Kobayashi K, Yokota T, Amino T, Owada K, Fujigasaki H, Sakamoto M, Tomimitsu H, Takashima M, Kumagai J, Noguchi Y, Kawashima Y, Ohkoshi N, Ishida G, Gomyoda M, Yoshida M, Hashizume Y, Saito Y, Murayama S, Yamanouchi H, Mizutani T, Kondo I, Toda T, Mizusawa H (2005) An autosomal dominant cerebellar ataxia linked to chromosome 16q22.1 is associated with a single-nucleotide substitution in the 5' untranslated region of the gene encoding a protein with spectrin repeat and Rho guanine nucleotide exchange-factor domains. *Am J Hum Genet* 77:280–296
- Koob MD, Moseley ML, Schut LJ, Benzow KA, Bird TD, Day JW, Ranum LP (1999) An untranslated CTG expansion causes a novel form of spinocerebellar ataxia (SCA8). *Nat Genet* 21:379–384
- Matsuura T, Yamagata T, Burgess DL, Rasmussen A, Grewal RP, Watase K, Khajavi M, McCall AE, Davis CF, Zu L, Achari M, Pulst SM, Alonso E, Noebels JL, Nelson DL, Zoghbi HY, Ashizawa T (2000) Large expansion of the ATTCT pentanucleotide repeat in spinocerebellar ataxia type 10. *Nat Genet* 26:191–194
- Nagaoka U, Takashima M, Ishikawa K, Yoshizawa K, Yoshizawa T, Ishikawa M, Yamawaki T, Shoji S, Mizusawa H (2000) A gene on SCA4 locus causes dominantly inherited pure cerebellar ataxia. *Neurology* 54:1971–1975
- Ohata T, Yoshida K, Sakai H, Hamanoue H, Mizuguchi T, Shimizu Y, Okano T, Takada F, Ishikawa K, Mizusawa H, Yoshiura K, Fukushima Y, Ikeda S, Matsumoto N (2006) A -16C>T substitution in the 5' UTR of the puratrophin-1 gene is prevalent in autosomal dominant cerebellar ataxia in Nagano. *J Hum Genet* 51:461–466
- Onodera Y, Aoki M, Mizuno H, Warita H, Shiga Y, Itoyama Y (2006) Clinical features of chromosome 16q22.1 linked autosomal dominant cerebellar ataxia in Japanese. *Neurology* 67:1300–1302
- Ouyang Y, Sakoe K, Shimazaki H, Namekawa M, Ogawa T, Ando Y, Kawakami T, Kaneko J, Hasegawa Y, Yoshizawa K, Amino T, Ishikawa K, Mizusawa H, Nakano I, Takiyama Y (2006) 16q-linked autosomal dominant cerebellar ataxia: a clinical and genetic study. *J Neurol Sci* 247:180–186
- Ross CA, Poirier MA (2004) Protein aggregation and neurodegenerative disease. *Nat Med* 10 Suppl:S10–S17
- Sasaki H, Yabe I, Tashiro K (2003) The hereditary spinocerebellar ataxias in Japan. *Cytogenet Genome Res* 100:198–205
- Schöls L, Bauer P, Schmidt T, Schulte T, Riess O (2004) Autosomal dominant cerebellar ataxias: clinical features, genetics, and pathogenesis. *Lancet Neurol* 3:291–304
- van Swieten JC, Brusse E, de Graaf BM, Krieger E, van de Graaf R, deKoning I, Maat-Kievit A, Leegwater P, Dooijes D, Oostra BA, Heutink P (2003) A mutation in the fibroblast growth factor 14 gene is associated with autosomal dominant cerebellar ataxia. *Am J Hum Genet* 72:191–199
- Takano H, Cancel G, Ikeuchi T, Lorenzetti D, Mawad R, Stevanin G, Didierjean O, Durr A, Oyake M, Shimohata T, Sasaki R, Koide R, Igarashi S, Hayashi S, Takiyama Y, Nishizawa M, Tanaka H, Zoghbi H, Brice A, Tsuji S (1998) Close associations between prevalences of dominantly inherited spinocerebellar ataxias with CAG-repeat expansions and frequencies of large normal CAG alleles in Japanese and Caucasian populations. *Am J Hum Genet* 63:1060–1066
- Takashima M, Ishikawa K, Nagaoka U, Shoji S, Mizusawa H (2001) A linkage disequilibrium at the candidate gene locus for 16q-linked autosomal dominant cerebellar ataxia type III in Japan. *J Hum Genet* 46:167–171
- Waters MF, Minassian NA, Stevanin G, Figueroa KP, Bannister JP, Nolte D, Mock AF, Evidente VG, Fee DB, Muller U, Durr A, Brice A, Papazian DM, Pulst SM (2006) Mutations in voltage-gated potassium channel KCNC3 cause degenerative and developmental central nervous system phenotypes. *Nat Genet* 38:447–451
- Wieczorek S, Arning L, Alheite I, Epplen JT (2006) Mutations of the puratrophin-1 (PLEKHG4) gene on chromosome 16q22.1 are not a common genetic cause of cerebellar ataxia in a European population. *J Hum Genet* 51: 363–367
- Yu GY, Howell MJ, Roller MJ, Xie TD, Gomez CM (2005) Spinocerebellar ataxia type 26 maps to chromosome 19p13.3 adjacent to SCA6. *Ann Neurol* 57:349–354

Direct and accurate measurement of CAG repeat configuration in the *ataxin-1* (*ATXN-1*) gene by “dual-fluorescence labeled PCR-restriction fragment length analysis”

Jiang X. Lin · Kinya Ishikawa · Masaki Sakamoto ·
Taiji Tsunemi · Taro Ishiguro · Takeshi Amino ·
Shuta Toru · Ikuko Kondo · Hidehiro Mizusawa

Received: 30 September 2007 / Accepted: 15 December 2007 / Published online: 27 February 2008
© The Japan Society of Human Genetics and Springer 2008

Abstract Spinocerebellar ataxia type 1 (SCA1; OMIM: #164400) is an autosomal dominant cerebellar ataxia caused by an expansion of CAG repeat, which encodes polyglutamine, in the *ataxin-1* (*ATXN1*) gene. Length of polyglutamine in the *ATXN1* protein is the critical determinant of pathogenesis of this disease. Molecular diagnosis of SCA1 is usually undertaken by assessing the length of CAG repeat configuration using primers spanning this configuration. However, this conventional method may potentially lead to misdiagnosis in assessing polyglutamine-encoding CAG repeat length, since CAT interruptions may be present within the CAG repeat configuration, not only in normal controls but also in neurologically symptomatic subjects. We developed a new method for assessing actual CAG repeat numbers not interrupted by CAT sequences. Polymerase chain reaction using a primer pair labeled with two different fluorescences followed by restriction enzyme digestion with SfaNI which recognizes the sequence “GCATC(N)₅”, lengths of actual

CAG repeats that encode polyglutamine were directly detected. We named this method “*dual fluorescence labeled PCR-restriction fragment length analysis*”. We found that numbers of actual CAG repeat encoding polyglutamine do not overlap between our cohorts of normal chromosomes ($n = 385$) and SCA1 chromosomes ($n = 5$). We conclude that the present method is a useful way for molecular diagnosis of SCA1.

Keywords SCA1 · PCR · RFLP (restriction fragment length polymorphism) · Molecular diagnosis · Polyglutamine disease · Ataxia · Mutation detection

Introduction

Spinocerebellar ataxia type 1 (SCA1) (OMIM: #164400) is caused by an expansion of trinucleotide (CAG) repeat that encodes polyglutamine tract in the *ataxin-1* (*ATXN1*) gene (OMIM: *601556) lying in the short arm of human chromosome 6 (6p23) (Chung et al. 1993; Orr et al. 1993; Banfi et al. 1994). In normal chromosomes, this CAG repeat shows repeat-length polymorphism ranging in size between 19 and 39 repeats. In contrast, the length of expanded CAG repeat in the SCA1 disease chromosomes ranges from 39 up to 81 repeats. The length of expansion is inversely correlated with age-of-onset of disease, suggesting a direct role of CAG repeat/polyglutamine length in the pathogenesis of SCA1 (Chung et al. 1993; Orr et al. 1993; Banfi et al. 1994).

The *ataxin-1* (*ATXN-1*) gene encodes a protein called ataxin-1 (ATXN-1), which is a 816-amino acid protein with a molecular mass of 87 kDa. The polyglutamine tract lies at its amino (N)-terminal region. In addition to the

Analysis of CAG repeats in the *ataxin-1* gene.

J. X. Lin · K. Ishikawa (✉) · M. Sakamoto · T. Tsunemi ·
T. Ishiguro · T. Amino · S. Toru · H. Mizusawa
Department of Neurology and Neurological Science,
Graduate School, Tokyo Medical and Dental University,
Yushima 1-5-45, Bunkyo-ku, Tokyo 113-8519, Japan
e-mail: kishikawa.nuro@tmd.ac.jp

I. Kondo
Department of Medical Genetics, Ehime University,
Onsen-gun, Ehime, Japan

Present Address:

I. Kondo
Ibaraki Prefectural Child Welfare Health Center,
Yoshizawa-cho 3979-3, Mito, Ibaraki 310-0845, Japan

polyglutamine tract, there are some other important domains in ATXN-1, such as nuclear localization signal and the AXH domains. Although the functions of ATXN-1 are not fully understood, recent investigation suggests that the AXH domain in the ATXN-1 interacts with Gfi-1/Senseless protein depending on the length of the polyglutamine tract, resulting in reduction of the Gfi-1 level, which in turn may contribute to neurodegeneration (Tsuda et al. 2005).

The molecular diagnosis of SCA1 is usually undertaken by PCR amplification using primer pairs spanning the CAG repeat (Matilla et al. 1993; Orr et al. 1993; Goldfarb et al. 1996). However, this conventional method may contain caveats mainly stemming from the presence of trinucleotide CAT interruption sequence(s) within the CAG repeat tract. Most (98%) of the normal alleles contain one to three CAT interruptions, resulting in a much shorter polyglutamine tract when it is translated. On the other hand, expanded CAG repeats are characterized by continuous, “pure” CAG stretches, resulting in pure polyglutamine expansions (Chung et al. 1993). This fact would imply that the diagnosis of SCA1 is important to assess, not merely by the length of “CAG repeat configuration” (i.e., total length of CAG and CAT repeats), but by determining the length of pure CAG repeat encoding polyglutamine. Indeed, some exceptional cases have been previously reported. An allele with 44 repeats, which indicates “expansion” in conventional method, has been reported in an asymptomatic subject (Quan et al. 1995). This subject harbored CAG repeat configuration of (CAG)₁₂CATCAGCAT (CAG)₁₂CATCAGCAT (CAG)₁₄, showing that this allele encodes for polyglutamine tract with normal length due to four CAT interruptions. Another example has been reported in an expanded allele with 58 repeats interrupted with two CAT sequences as, 5'-(CAG)₄₅CATCAGCAT(CAG)₁₀-3' (Matsuyama et al. 1999). Particularly, special caution would be needed when assessing the CAG repeat length near the border of normal and expanded repeats, since the upper limit of normal repeat and the shortest expansion overlap at 38 repeats. While “pure” 38 CAG stretch is pathogenic, the 38 CAG repeat with CAT interruption is not pathogenic due to the much shorter polyglutamine stretch (Ranum et al. 1994). From these observations, it would be better if one could directly assess the actual CAG repeat length not interrupted by CAT sequences, since the length of polyglutamine tract in the ATXN-1 is the only basic defect that leads to pathogenesis.

In this study, we developed a new method that would allow one to detect the actual number of CAG repeat length not interrupted by CAT sequence(s). We show here that, by using our new method, one can directly assess 5'- and 3'-CAG repeat numbers disrupted by CAT sequence(s) which

may be contained in the CAG repeat configuration. We propose that this new method, “dual fluorescence labeled PCR-restriction fragment length analysis”, is a direct way to accurately diagnose SCA1. We not only introduce this new method, but we also show that actual “pure” CAG repeat numbers do not overlap between normal Japanese and SCA1 subjects by using this method. We also describe a unique family with short, but pathogenic, CAG repeats detected with our new method.

Materials and methods

Overall design of the dual fluorescence labeled PCR-restriction fragment length analysis

As previously described by others (Chung et al. 1993), every CAT interruption within “the CAG repeat configuration” (i.e., total length of CAG and CAT repeats) is theoretically recognized and digested with the restriction enzyme, “SfaNI”, which recognizes 5'-GCATC(N)₅-3'. There are no other consensus SfaNI sites outside the CAG repeat configuration when the genome is amplified using appropriate primers. Using this advantage, we designed a comparison of fragment lengths of the PCR product both with and without the SfaNI digestion (Fig. 1).

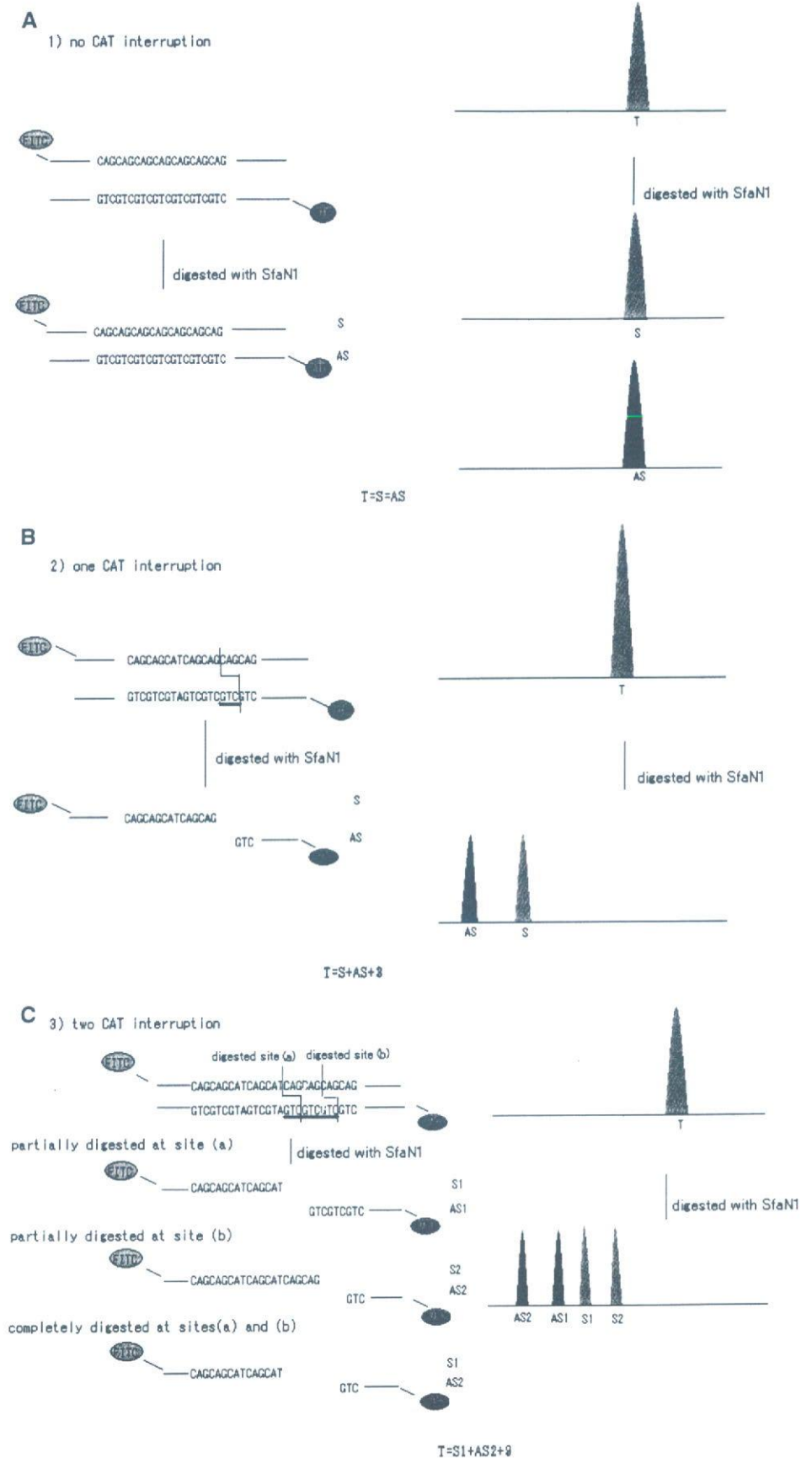
When there are no CAT interruptions within the CAG repeat configuration, the fragment length after SfaNI digestion will theoretically be the same as that without digestion (Fig. 1A).

When there is one CAT interruption, the length of the PCR product without the digestion would be calculated as the sum of lengths of two different fragments yielded after the digestion: the sum of the lengths of “the 5'-digested fragment”, “the 3'-digested fragment”, and 3 (Fig. 1B). The 5'- and 3'- SfaNI digested fragments could be differentiated if the sense and anti-sense primers are labeled with different fluorescent dyes.

When there are two CAT interruptions, the length of the PCR product without the digestion would be calculated as the sum of lengths of three different fragments yielded after the digestion: “5'-digested fragment”, “GCATC(N)₅”, and “the 3'-digested fragment” (Fig. 1C). Conversely, the size difference between fragment length without the digestion and the sum of “5'-digested fragment” and “the 3'-digested fragment”, would be the length of “GCATC(N)₅”.

CAG repeat configurations containing more than two CAT interruptions were not seen in our cohort of samples (data shown in Results). We therefore artificially generated such clones using site-directed mutagenesis (Invitrogen, Calif., USA). When there are more than two CAT interruptions, the length of PCR fragments without the enzyme digestion “minus” the sum of lengths of the 5'- and 3'-

Fig. 1 A basic concept of the dual-fluorescence labeled PCR-restriction fragment length analysis. *T* Length of PCR product containing whole CAG repeat configuration. *S* Fragment length of 5' sense-strand PCR product, labeled by FITC (fluorescence isothiocyanate) yielded after restriction enzyme SfaNI, digestion. *AS* Fragment length of 3' anti-sense-strand PCR product labeled by VIC yielded after restriction enzyme SfaNI, digestion. **A** In case of no CAT interruption in the CAG repeat configuration, PCR fragment without SfaNI (*T*), 5' sense-strand PCR product labeled by FITC yielded after SfaNI digestion (*S*), and the 3' anti-sense-strand PCR product labeled by VIC yielded after SfaNI digestion (*AS*) all coincide in length on ABI PRISM 3100-Avant System. **B** In case one, CAT interruption is present within the CAG repeat configuration. The length of PCR fragment without SfaNI (*T*) is calculated as the sum of (5' sense-strand PCR product labeled by FITC yielded after SfaNI digestion: *S*), (3' anti-sense-strand PCR product labeled by VIC yielded after SfaNI digestion: *AS*), and 3 base-pair (bp) due to trinucleotide, GTC, on anti-sense strand (*underlined*). $T = S + AS + 3$ (bp). **C** In case two, CAT interruptions are present within the CAG repeat configuration. Two different SfaNI-digestion sites (*a* and *b*) are predicted (*right panel*). Theoretically, four types of fragments would be yielded due to combination of complete and partial digestions (two FITC-labeled fragments, *S1* and *S2*, and two VIC-labeled fragments, *AS1* and *AS2*). The length of PCR fragment without SfaNI (*T*) could be calculated as the sum of $S1 + AS2 + 9$ bp (corresponding nine-nucleotide "GTCGTCGTC", *underlined* in *right panel*)



SfaNI digested fragments would be the differences harboring CAT interruptions.

Thus, it seemed theoretically possible to detect both 5'- and 3'-CAG repeat sequences disrupted by CAT interruption. We tested our hypothesis first by examining 10 plasmid clones containing *ATXN1* CAG repeat configurations obtained from five individuals (Table 1).

DNA samples and materials

One hundred and ninety-one control individuals and two SCA1 subjects were first analyzed. The control group comprised of 60 neurologically normal subjects, 50 subjects with cerebrovascular diseases, in whom no family history of ataxia was present, and 81 individuals with dominantly inherited ataxias previously excluded for SCA1 by conventional diagnostic method. Two subjects with typical clinical features of SCA1 had been molecularly confirmed as having this disease by the conventional method. Peripheral blood samples were obtained after informed consent, and DNA was extracted as reported elsewhere (Ishikawa et al. 1997). The study was approved by the Institutional Review Board of Tokyo Medical and Dental University.

Detection of CAG repeat/CAT interruption with automated fluorescence sequencer

For amplifying the CAG repeat configuration, a primer set "CAG-a and CAG-b" (Chung et al. 1993) was used, although the sense primer was labeled with FITC (fluorescent isothiocyanate) at its 5'-end (CAG-b: 5'-[FITC]CCAGACGCCGGGACACAAGGCTGAG-3'), and the anti-sense primer was 5'-end labeled with VIC (CAG-a: 5'-[VIC]-CCGGAGCCCTGCTGAGGTG-3'). PCR was performed in an ordinary condition in a final volume of 25 μ l, containing 50 ng of genomic DNA, 4.0 pmol of each

primer, 1 μ l of 10% dimethylsulfoxide (DMSO), 2 mM each deoxynucleosides (dNTPs), and 1.0 unit of Gold Tag DNA polymerase (Takara, Japan). Thermal setting was initial denature at 95°C for 4 min, 3 cycles of 95°C for 1 min, 70°C for 30 s, 72°C for 30 s; subsequent 3 cycles of 95°C for 1 min, 68°C for 30 s, 72°C for 30 s; 3 cycles of 95°C for 1 min, 66°C for 30 s, 72°C for 30 s; 3 cycles of 95°C for 1 min, 64°C for 30 s, 72°C for 30 s; final 20 cycles of 95°C for 1 min, 62°C for 30 s, 72°C for 30 s, and final extension at 72°C for 10 min. For each reaction, 10 μ l of PCR product was digested with SfaNI (New England BioLabs, USA) in a final volume of 15 μ l containing optimal reaction condition (10 mM sodium chloride, 5 mM Tris-hydrochloride, 1 mM Mg Cl₂, 0.1 mM dithiothreitol (DTT; pH 7.9) incubated at 37°C, as recommended by the supplier (Chung et al. 1993). PCR products both with and without the SfaNI digestion were diluted with the same solution (Hi-Di Formamide and Gene Scan-500 LIZ Size Standard), and then heated at 95°C for 2 min for denature, immediately cooled within ice, and loaded on ABI PRISM 3100-Avant System (Applied Biosystems). The electrophoresis was undertaken at 50°C, with 15 volts.

Evaluation of dual fluorescence labeled PCR-restriction fragment length analysis

We first randomly chose five individuals with different CAG repeat configurations (Table 1). On each subject, genomic DNA was amplified with CAG-a and -b primers, and PCR product was subcloned into PCR-TOPO (Invitrogen, USA). Then, 10 clones from each individual were sequenced with universal and reverse primers as previously described (Li et al. 2003). These five individuals harbored any of the CAG repeat configurations without CAT interruption, or 1–2 CAT interruption(s). Then, the dual fluorescent-labeled PCR-restriction fragment length analysis was performed on these clones to check the consistency.

Results

Evaluation of dual fluorescence labeled PCR-restriction fragment length analysis

To evaluate consistency of our new method, we first examined on 10 plasmid clones which contained CAG repeat configuration in the *ATXN1* gene (Table 1). On the plasmid clones without CAT interruption within the CAG repeat configuration (e.g., Case 1, Allele 1), there were no differences in fragment lengths on ABI 3100-Avant System between data with and without the SfaNI restriction enzyme digestion (Fig. 1A), as has been hypothesized.

Table 1 The sequence configurations of 10 alleles derived from five control individuals and subcloned into pCR-TOPO plasmid vector

Case 1	Allele 1	(CAG)22
	Allele 2	(CAG)13CATCAGCAT (CAG)10
Case 2	Allele 1	(CAG)13CATCAGCAT (CAG)10
	Allele 2	(CAG)11CAT (CAG)16
Case 3	Allele 1	(CAG)11CAT (CAG)16
	Allele 2	(CAG)11CAT (CAG)16
Case 4	Allele 1	(CAG)13CATCAGCAT (CAG)10
	Allele 2	(CAG)13CATCAGCAT (CAG)10
Case 5	Allele 1	(CAG)11CAT (CAG)16
	Allele 2	(CAG)16CATCAGCAT (CAG)10

When plasmids with one CAT interruption were examined (e.g., Table 1, Case 2, Allele 2), the fragment length of the PCR product amplified by the two primers should be the sum of the lengths of “5′-digested fragment labeled with FITC”, that of “3′-digested fragment labeled with VIC”, and 3. The SfaNI digestion yielded was two fragments exactly corresponding the 5′-digested fragment labeled with FITC and the 3′-digested fragment labeled with VIC (Fig. 1B).

If the CAG repeat configuration contained two CAT interruptions, the PCR product should be separated into three fragments: “5′-digested fragment labeled with FITC”, “3′-digested fragment labeled with VIC”, and the “internal fragment limited by the two SfaNI-recognition sites”. Since this internal fragment is not labeled, this fragment will not be detected. However, the length of the “internal fragment limited by the two SfaNI-recognition sites” could be calculated by the following formula: (the length of internal sequence between the two CAT interruptions) = (the length of PCR product without SfaNI digestion) – (the sum of lengths of “5′-digested fragment labeled with FITC” and “3′-digested fragment labeled with VIC”). This was indeed confirmed by the experiment on plasmids with two CAT interruptions (e.g., Table 1, Case 4, Allele 1) with the dual fluorescence labeled PCR-restriction fragment length analysis (Fig. 1C).

These examinations not only confirmed our hypothesis, but also suggested that the new method is able to directly assess nucleotide sequences of CAG repeat configuration. If the length-difference between the fragments yielded with and without the SfaNI restriction enzyme digestion was nine nucleotide long, the nucleotide excised by the SfaNI was always as “5′-CATCAGCAT-3′”, confirmed by experiments on plasmid clones. Similarly, if the length-difference was 12 nucleotides, the internal sequence was always as “5′-CAT(CAG)₂CAT-3′”. If the lengths was 15 nucleotides, the internal sequence was always as “5′-CAT(CAG)₃CAT-3′”.

We did not find DNA samples with more than two CAT interruptions with the CAG repeat configuration in our cohort of 191 control subjects (data described later). To check the usefulness of our new method for alleles with more than two CAT interruptions, a CAG repeat configuration with three CAT interruptions was artificially generated from a plasmid clone, Case 5 Allele 2 (Table 1), by using site-directed mutagenesis. The exact sequence of this configuration containing three CAT interruption was “5′-(CAG)₉CAT(CAG)₆CATCAGCAT(CAG)₁₀-3′”. When digested with SfaNI, three fragments corresponding 5′-completely digested fragment labeled with FITC, 3′-completely digested fragment labeled with VIC, and 3′-partially digested fragment labeled with VIC, were detected (Fig. 2). The combined length of the 5′-completely

digested fragment labeled with FITC (S1) and the 3′-completely digested fragment labeled with VIC (AS2) was 18 base-pairs (bp) shorter than the length of total CAG repeat configuration, consistent with the fact that six CAG repeats were lying between two CAT interruption sequences.

Based on these observations, we confirmed that the dual fluorescence labeled PCR-restriction fragment length analysis appeared to be a useful and rapid way to directly assess CAG repeat configuration.

Results on 191 control individuals and two clinically typical SCA1 subjects

We next examined 191 control Japanese individuals and two SCA1 subjects by the dual fluorescence labeled PCR-restriction fragment length analysis. The two most frequent CAG repeat configurations were those with 26 and 28 combined CAG and CAT repeats (Fig. 3). The frequencies of these alleles in normal Japanese chromosomes were 27.1% for 28 CAG/CAT repeat-units, and 24.0% for 26 CAG/CAT repeat-units. The range of CAG repeat configuration was from 17 up to 40 repeat-units in control groups. Two SCA1 subjects harbored 46 and 54 repeat-units on their SCA1 chromosomes.

When 386 chromosomes from 193 individuals were examined by the dual fluorescence labeled PCR-restriction fragment length analysis, we found that 140 chromosomes had one CAT interruption with the CAG repeat configuration, counting 36.4% of our cohort of Japanese control chromosomes (Table 2). On the other hand, there were 243 chromosomes with two CAT interruptions, counting 62.9% of 386 chromosomes. Table 3 shows exact sequences of CAG repeat configurations that contain either 1 or 2 CAT interruption found in this study. There were seven chromosomes which did not contain CAT interruptions. Two of these were from SCA1 subjects with pure CAG expansions (46 and 54 CAG repeat-units) and typical clinical features. The remaining five chromosomes were observed from control subjects without ataxia. The frequency of normal CAG repeat length with pure stretch was calculated as 1.3%. The relation between the length of CAG repeat configuration (i.e., combined CAG and CAT repeats) and presence/absence of CAT interruptions is summarized in Table 2 (Note: this table includes three atypical SCA1 subjects, as described later. Therefore, the total number of chromosomes becomes 390, the number of normal chromosomes is 385, and the number of SCA1 chromosomes is five). Of note is that we did not find any alleles with three CAT interruptions.

When the SfaNI digestion was performed in the dual fluorescence labeled PCR-restriction fragment length

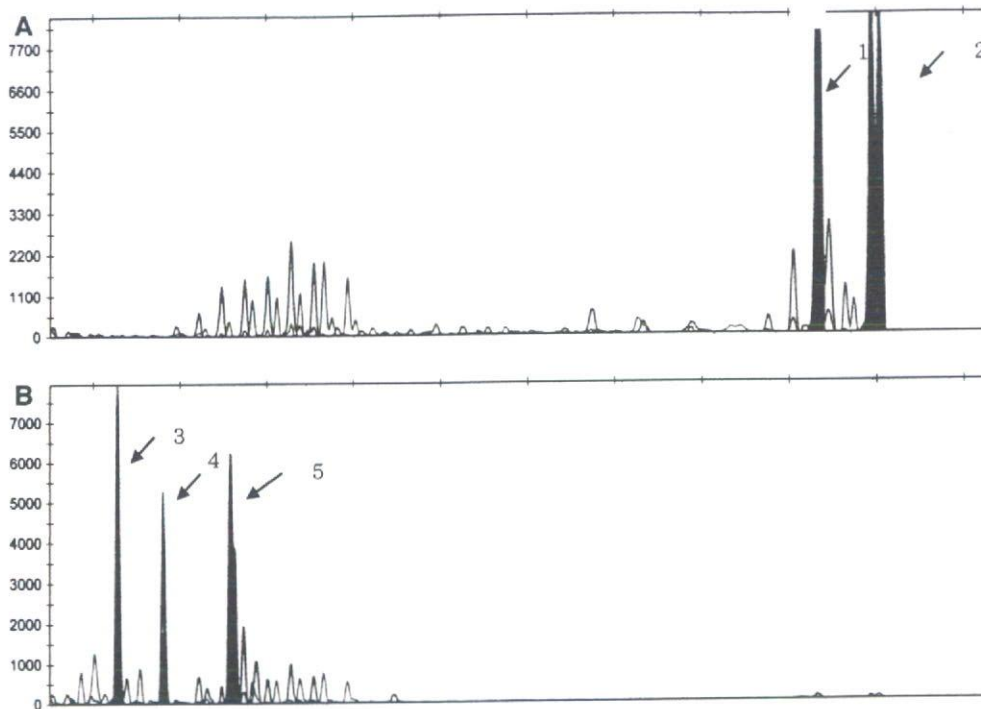


Fig. 2 The electrophoresis pattern of the dual-fluorescence labeled PCR-restriction fragment length analysis on a plasmid clone containing three CAT interruptions. **A** The fragment analysis on ABI 3100 without SfaNI digestion. FITC-labeled PCR product (arrow #1) and VIC-labeled PCR product (arrow #2) which are actually the same size in length, differ in size for 5.8 base-pairs (bp) on this analyzing system. This 5.8-bp gap between the FITC and VIC fragments was always constantly seen on ABI 3100. **B** The fragment analysis after SfaNI digestion. Three major peaks corresponding to a completely digested VIC-labeled 3' anti-sense-strand PCR fragment (arrow #3; designated, AS2), a partially digested, VIC-labeled 3' anti-

sense-strand PCR fragment (arrow #4; designated, AS1), and a completely digested, FITC-labeled 5' sense-strand PCR product (arrow #5; designated, S1), are demonstrated. When a total length of PCR fragment containing whole CAG repeat configuration is designated "T", $T = AS1 + AS2 + S1 + 18$ (bp) was confirmed both by fragment length analysis and actual sequence analysis. Although presence of a partially digested FITC-labeled 5' anti-sense-strand PCR fragment (designated, S2) has been considered on hypothesis, it was never observed on ABI3100 sequencer. Therefore, we considered that FITC-labeled PCR product directly reflects a completely digested fragment (S1)

analysis, we were able to determine where CAT interruptions were present in the CAG repeat configuration (Fig. 3B). The CAG repeat length in the FITC-labeled 5' fragment ranged in length from 10 up to 20 repeats in control chromosomes. This would indicate that the normal CAG repeat-unit lying in the 5'-region of the CAT interruption ranges between 10 and 20. Similarly, the CAG repeat length in the VIC-labeled 3' fragment ranged in length from 7 to 23 repeats (Table 3).

Identification of a family with 40 CAG repeats with interruption

In our series of examining 193 individuals by the dual fluorescence labeled PCR-restriction fragment length analysis, we encountered an individual who harbored an allele with very small CAG repeat expansion. The size of this allele was 40 combined CAG and CAT repeats, which could be diagnosed as SCA1 by the classical criteria. By the dual fluorescent labeled PCR-restriction fragment

length analysis, however, the repeat configuration was suggested to have two CAT interruptions with 27 CAG repeats in the 5'-end, and 10 CAG repeats in the 3'-end ("5'-CAG₂₇CATCAGCATCAG₁₀-3'"). When the PCR product was sub-cloned into PCR-TOPO and sequenced, the allele with 40 CAG repeat configuration was confirmed to harbor two CAT interruptions as expected from the dual fluorescent labeled PCR-restriction fragment length analysis. From the distribution pattern of actual CAG repeat number found in control Japanese (Fig. 3B), we considered that this particular individual had an abnormal SCA1 allele.

This patient was a 47-year-old male subject showing gait disturbance due to marked spastic paraparesis and mild truncal ataxia. He first noticed difficulties in walking at the age of 43. He had two elder siblings with similar neurological symptoms. The patient's mother, who died at the age of 75, also showed progressive gait disturbance beginning from her fourth decade. Although a DNA sample of this mother was not available for examination, DNA samples of the patient's siblings were tested and were both confirmed to have the same allele with "5'-

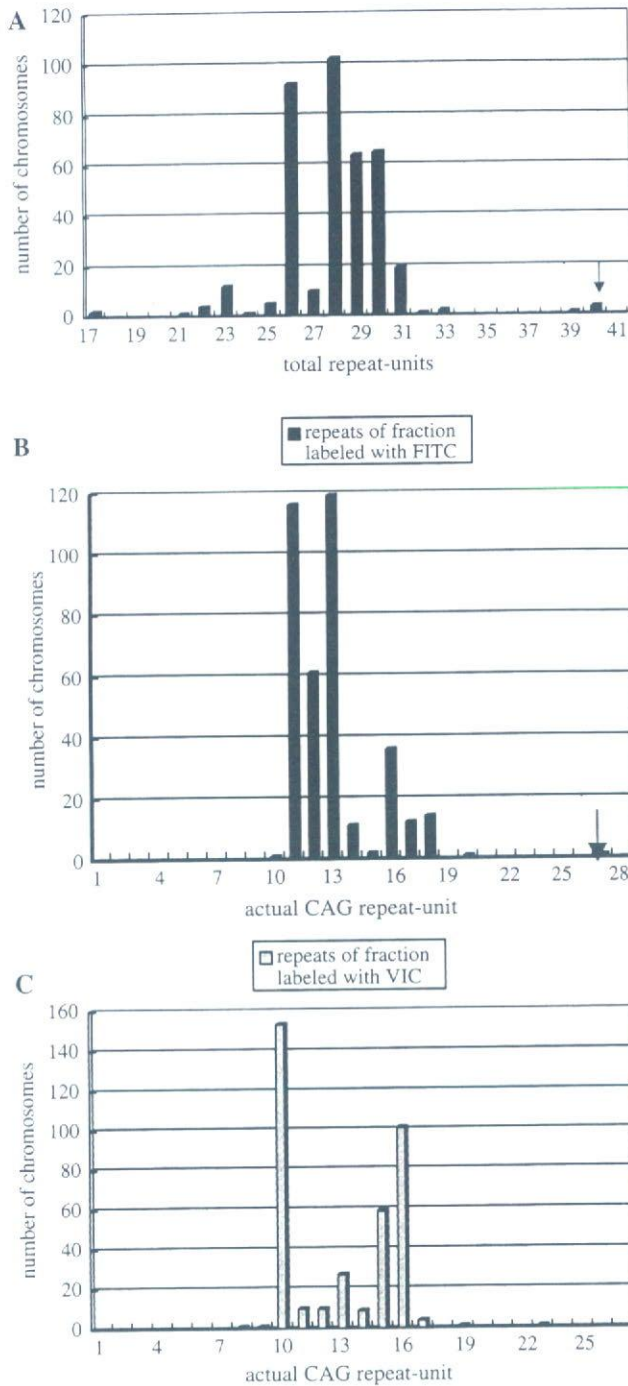


Fig. 3 The analysis of the SCA1 CAG repeats in control Japanese individuals. **A** The distribution of CAG repeat configuration (i.e., combined CAG repeat and CAT interruptions). In the present cohort of 193 Japanese subjects, the CAG repeat number which may contain CAT interruptions ranged from 17 to 40 repeat-unit. **B** The distribution of actual (pure) CAG repeat number encoding polyglutamine in the region 5' (upstream) of the first CAT interruption. Pure CAG repeat in the 5'-region ranges from 10 to 20 repeat-units, and two major peaks are seen at 11 and 13 CAG repeats. Notice that a chromosome with 27 pure CAG repeat was an exceptionally large repeat. **C** The distribution of actual (pure) CAG repeat number encoding polyglutamine in the region 3' (downstream) of the last CAT interruption. Pure CAG repeat in the 3'-region ranges from 7 to 23 repeat-units, and two major peaks are seen at 10 and 16 CAG repeats

Table 2 The distribution of CAT interruption among various CAG repeats in the present study

Length of allele	Pure CAG repeats	One CAT interruption	Two CAT interruptions
17	2		
21		1	
22	2	1	1
23	1	10	1
24			1
25		2	3
26		13	81
27		8	2
28		88	15
29		7	58
30		7	58
31		1	18
32		1	
33			2
39		1	
40			3
46	1		
54	1		
Total	7	140	243

(data shown upon request). From these observations, we conclude that spastic ataxia phenotype in these patients carrying 40 CAG repeat configuration ("5'-CAG₂₇CAT-CAGCATCAG₁₀-3'") may be caused by a mild CAG repeat expansion in the *ATXN1* gene.

CAG₂₇CATCAGCATCAG₁₀-3'". Magnetic resonance imaging of the brain and the cervical, thoracic and lumbar spinal cord of these three subjects revealed mild cerebellar atrophy without obvious spinal cord or brainstem atrophy, which is compatible with SCA1 (Burk et al.1996). We also tested for mutations in *spastin* gene (Proukakis et al.2003), the most common gene identified for autosomal dominant spastic paraplegia (Svenson et al.2001). However, there was no mutation at least in the coding region of this gene

Discussion

The main fruit of this study is the development of a new diagnostic method that would allow ones to detect actual CAG repeat numbers and the number of CAT interruptions in the CAG repeat configuration. The conventional method using a primer pair flanking CAG repeat configuration

Table 3 CAG repeat configurations with CAT interruptions in the present study

Length of allele	Number of alleles	The sequence configurations with one CAT interruption	Number of alleles	The sequence configurations with two CAT interruption
21	1	5'-CAG ₁₁ CATCAG ₉ -3'		
22	1		1	5'-CAG ₁₁ CATCAGCATCAG ₈ -3'
23	10	5'-CAG ₁₁ CATCAG ₁₁ -3'	1	5'-CAG ₁₀ CATCAGCATCAG ₁₀ -3'
24			1	5'-CAG ₁₁ CATCAGCATCAG ₁₀ -3'
25	2	5'-CAG ₁₁ CATCAG ₁₆ -3'	3	5'-CAG ₁₂ CATCAGCATCAG ₁₀ -3'
26	13	5'-CAG ₁₃ CATCAG ₁₂ -3'	81	5'-CAG ₁₃ CATCAGCATCAG ₁₀ -3'
27	8	5'-CAG ₁₁ CATCAG ₇ -3'	2	5'-CAG ₁₄ CATCAGCATCAG ₁₀ -3'
28	80	5'-CAG ₁₁ CATCAG ₁₆ -3'	15	5'-CAG ₁₄ CATCAGCATCAG ₁₁ -3'
	8	5'-CAG ₁₂ CATCAG ₁₅ -3'		
29	3	5'-CAG ₁₃ CATCAG ₁₅ -3'	19	5'-CAG ₁₃ CATCAGCATCAG ₁₃ -3'
	2	5'-CAG ₁₂ CATCAG ₁₆ -3'	38	5'-CAG ₁₆ CATCAGCATCAG ₁₀ -3'
	1	5'-CAG ₁₄ CATCAG ₁₄ -3'	1	5'-CAG ₁₂ CATCAGCATCAG ₁₄ -3'
	1	5'-CAG ₁₈ CATCAG ₁₀ -3'		
30	5	5'-CAG ₁₃ CATCAG ₁₆ -3'	42	5'-CAG ₁₅ CATCAGCATCAG ₁₂ -3'
	2	5'-CAG ₁₂ CATCAG ₁₉ -3'	6	5'-CAG ₁₄ CATCAGCATCAG ₁₃ -3'
			10	5'-CAG ₁₇ CATCAGCATCAG ₁₀ -3'
31	1	5'-CAG ₁₈ CATCAG ₁₂ -3'	14	5'-CAG ₁₈ CATCAGCATCAG ₁₀ -3'
			1	5'-CAG ₁₅ CATCAGCATCAG ₁₃ -3'
			2	5'-CAG ₁₆ CATCAGCATCAG ₁₂ -3
			1	5'-CAG ₁₇ CATCAGCATCAG ₁₁ -3'
32	1	5'-CAG ₁₂ CATCAG ₁₉ -3'		
33			1	5'-CAG ₂₀ CATCAGCATCAG ₁₀ -3'
			1	5'-CAG ₁₆ CATCAGCATCAG ₁₄ -3
39	1	5'-CAG ₁₅ CATCAG ₂₃ -3'		
40			3	5'-CAG ₂₇ CATCAGCATCAG ₁₀ -3'
Total	140		243	

allowed one to measure total CAG and CAT repeat-units (Goldfarb et al. 1996; Jodice et al. 1997; Matsuyama et al. 1999; Pujana et al. 1999; Zhulke et al. 2002).

Sobczak and Krzyzosiak (2004) developed a new method, "SSCP-duplex analysis", and showed exact CAG repeat configurations in 50 Polish individuals. Hellenbroich and his colleague developed a method that would detect actual CAG repeat by using non-labeled primers and SfaNI digestion (Zhulke et al. 2002). They studied in their German population and found rare alleles with mild CAG repeat expansion. However, their method would not discriminate 5'-end SfaNI-digested fragment with 3'-end SfaNI-digested fragment, and would need another step to disclose true CAG repeat configuration. In contrast, our method could allow one to discriminate both 5'- and 3'-fragments by labeling sense and anti-sense primers with different fluorescent dyes. Therefore, it would be much convenient and accurate to determine actual CAG repeat-unit encoding polyglutamine tract by employing our dual fluorescence labeled PCR-restriction fragment length analysis on fluorescence sequencers.

By using this new method, we have shown CAG repeat configurations in 385 control Japanese chromosomes and five SCA1 patients chromosomes. As has been reported in many studies, most of the normal chromosomes (98.7%) contain at least one CAT interruption in the CAG repeat configuration (Chung et al. 1993). However, we also found that 5 out of 385 (1.3%) control Japanese chromosomes do not contain the interruption. Since presence of CAT interruptions is considered to stabilize the CAG repeat length, presence of normal alleles without the CAT interruption may have some effect in the emergence of CAG repeat expansion through transmission. Comparing repeat numbers of CAG repeat configuration with and without CAT interruptions, alleles with interruption tended to have longer CAG repeat. In other words, it was not clear whether pure CAG repeat expansion occurs from the normal CAG repeat without CAT interruption.

In conclusion, the present method could be a convenient way to detect the accurate number of CAG repeat-unit encoding polyglutamine tract. The usefulness would be

particularly important for CAG repeats with borderline length.

References

- Banfi S, Servadio A, Chung MY, Kwiatkowski TJ Jr, McCall AE, Duvick LA, Shen Y, Roth EJ, Orr HT, Zoghbi HY (1994) Identification and characterization of the gene causing type 1 spinocerebellar ataxia. *Nat Genet* 7:513–520
- Burk K, Abele M, Fetter M, Dichgan J, Skalej M, Laccone F, Didierjean O, Brice A, Klockgether T (1996) Autosomal dominant cerebellar ataxia type I clinical features and MRI in families with SCA1, SCA2 and SCA3. *Brain* 119(Pt 5):1497–1505
- Chung M-Y, Ranum LPW, Duvick LA, Servadio A, Zoghbi HY, Orr HT (1993) Evidence for a mechanism predisposing to intergenerational CAG repeat instability in spinocerebellar ataxia type 1. *Nat Genet* 5:254–258
- Quan F, Janas J, Poppvich BW (1995) A novel CAG repeat configuration in the SCA1 gene: implications for the molecular diagnostics of spinocerebellar ataxia type 1. *Hum Mol* 4:2411–2413
- Goldfarb LG, Vasconcelos O, Platonov FA, Lunke A, Kipnis V, Kononova S, Chabrashvili T, Vlasimirtsev VA, Alexeev VP, Gajdusek DC (1996) Unstable triplet repeat and phenotypic variability of spinocerebellar ataxia type 1. *Ann Neurol* 39:500–506
- Ishikawa K, Tanaka H, Saito M, Ohkoshi N, Fujita T, Yoshizawa K, Ikeuchi T, Watanabe M, Hayashi A, Takiyama Y, Nishizawa M, Nakano I, Matsubayashi K, Miwa M, Shoji S, Knazawa I, Tsuji S, Mizusawa H (1997) Japanese families with autosomal dominant pure cerebellar ataxia map to chromosome 19p13.1–p13.2 and are strongly associated with mild CAG expansions in the spinocerebellar ataxia type 6 gene in chromosome 19p13.1. *Am J Hum Genet* 61(2):336–346
- Jodice C, Giovannone B, Calabresi V, Bellocchi M, Terrenato L, Novelletto A (1997) Population variation analysis at nine loci containing expressed trinucleotide repeats. *Ann Hum Genet* 61:425–438
- Li M, Ishikawa K, Toru S, Tomimitsu H, Takashima M, Goto J, Takiyama Y, Sasaki H, Imoto I, Inazawa J, Toda T, Kanazawa I, Mizusawa H (2003) Physical map and haplotype analysis of 16q-linked autosomal dominant cerebellar ataxia (ADCA) type III in Japan. *Am J Hum Genet* 48(3):111–118
- Matilla T, Volpini V, Genis D, Rosell J, Corral J, Dávalos A, Molins A, Estivill X (1993) Presymptomatic analysis of spinocerebellar ataxia type 1 (SCA1) via the expansion of the SCA1 CAG repeat in a large pedigree displaying anticipation and parental male bias. *Hum Mol Genet* 2:2123–2128
- Matsuyama Z, Izumi Y, Kameyama M, Kawakami H, Nakamura S (1999) The effect of CAT trinucleotide interruptions on the age at onset of spinocerebellar ataxia type 1 (SCA1). *J Med Genet* 36:546–548
- Orr H, Chung M-Y, Banfi S, Kwiatkowski TJ Jr, Servadio A, Beaudet AL, McCall AE, Duvick LA, Ranum LPW, Zoghbi HY (1993) Expansion of an unstable trinucleotide CAG repeat in spinocerebellar ataxia type 1. *Nat Genet* 4:221–226
- Proukakis C, Auer-Grumbach M, Wagner K, Wilkinson PA, Reid E, Patton MA, Warner TT, Crosby AH (2003) Screening of patients with hereditary spastic paraplegia reveals seven novel mutations in the *SPG4* (Spastin) gene. *Hum Mutat* 21(2):170
- Pujana MA, Corral J, Gratacos M, Combarros O, Berciano J, Genis D, Banchs I, Estivill X, Volpini V (1999) Spinocerebellar ataxias in Spanish patients: genetic analysis of familial and sporadic cases. The ataxia study group. *Hum Genet* 104:516–522
- Ranum LP, Chung M-Y, Banfi S, Bryer A, Schut LJ, Ramesar R, Duvick LA, McCall A, Subramony SH, Goldfarb L, Gomez C, Sandkuijl LA, Orr HT, Zoghbi HY (1994) Molecular and clinical correlations in spinocerebellar ataxia type 1: evidence for familial effects on the age at onset. *Am J Hum Genet* 55:244–252
- Sobczak K, Krzyzosiak WJ (2004) Pattern of CAG repeat interruptions in SCA1 and SCA2 genes in relation to repeat instability. *Hum Mutat* 24:236–247
- Svenson IK, Ashley-Koch AE, Gaskell PC, Riney TJ, Cumming WJ, Kingston HM, Hogan EL, Boustany RM, Vance JM, Nance MA, Pericak-Vance MA, Marchuk DA (2001) Identification and exoexpression analysis of spastin gene mutation in hereditary spastic paraplegia. *Am J Hum Genet* 68(5):1077–85
- Tsuda H, Jafar-Nejad H, Patel AJ, Sun Y, Chen HK, Rose MF, Venken KJ, Botas J, Orr HT, Bellen HJ, Zoghbi HY (2005) The AXH domain of Ataxin-1 mediates neurodegeneration through its interaction with Gif-1/senseless proteins. *Cell* 122:633–644
- Zhulke C, Dalski A, Hellenbroich Y, Bubel S, Schwinger E, Burk K (2002) Spinocerebellar ataxia type 1 (SCA1): phenotype-genotype correlation studies in intermediate alleles. *Eur J Hum Genet* 10:204–209

Bax-inhibiting peptide protects cells from polyglutamine toxicity caused by Ku70 acetylation

Y Li^{1,5}, T Yokota^{*,1,5}, V Gama², T Yoshida^{1,2}, JA Gomez², K Ishikawa¹, H Sasaguri¹, HY Cohen³, DA Sinclair⁴, H Mizusawa¹ and S Matsuyama^{*,2}

Polyglutamine (polyQ) diseases, such as Huntington's disease and Machado–Joseph disease (MJD), are caused by gain of toxic function of abnormally expanded polyQ tracts. Here, we show that expanded polyQ of ataxin-3 (Q79C), a gene that causes MJD, stimulates Ku70 acetylation, which in turn dissociates the proapoptotic protein Bax from Ku70, thereby promoting Bax activation and subsequent cell death. The Q79C-induced cell death was significantly blocked by Ku70 or Bax-inhibiting peptides (BIPs) designed from Ku70. Furthermore, expression of SIRT1 deacetylase and the addition of a SIRT1 agonist, resveratrol, reduced Q79C toxicity. In contrast, mimicking acetylation of Ku70 abolished the ability of Ku70 to suppress Q79C toxicity. These results indicate that Bax and Ku70 acetylation play important roles in Q79C-induced cell death, and that BIP may be useful in the development of therapeutics for polyQ diseases.

Cell Death and Differentiation (2007) 14, 2058–2067; doi:10.1038/sj.cdd.4402219; published online 21 September 2007

Nine inherited neurodegenerative disorders with expanded polyglutamine (polyQ) are caused by mutations in different genes, but they likely share the common pathology in which expanded polyQ gains toxic functions.¹ The molecular mechanism of neuronal toxicity of polyQ remains enigmatic. Recent findings suggest that the intracellular aggregation of polyQ causes cellular stress responses that trigger neuronal cell death.¹ It is hypothesized that polyQ aggregation suppresses neuronal transcriptional activity by sequestering histone acetyltransferases (HAT) from chromosomes and thus polyQ causes neuronal cell death.^{2–4}

Bax is a proapoptotic member of Bcl-2 family proteins that plays a key role in programmed cell death in neurons.^{5,6} Recently, mutant huntingtin with expanded polyQ was shown to activate p53 and increase the expression level of Bax.⁷ Based on these previous findings, we became interested in examining the role of Bax in polyQ-induced cell death. Recently, we developed a series of cytoprotective membrane-permeable pentapeptides that rescue cells from Bax-mediated cell death. These peptides are named Bax-inhibiting peptides (BIPs) and were designed from the Bax binding domain of Ku70.^{8–10} Ku70 is a multifunctional protein playing roles in DNA repair and cell survival.¹¹ Ku70 has been shown to inhibit Bax-mediated cell death by binding Bax in the cytosol.^{12–14} The present study demonstrates that BIP can rescue cells from polyQ toxicity, and that polyQ promotes Bax-mediated cell death by inducing Ku70 acetylation that activates Bax.

Results

BIP suppresses Q79C-induced cell death. BIPs consisting of five amino acids (e.g. VPMLK and VPTLK) were used in this study. A mutated peptide (i.e. IPMIK) that does not bind Bax but retains cell permeability was also used in this study as a negative control (NC). For the investigation of polyQ toxicity, we used the C-terminal, truncated fragment of the Machado–Joseph disease 1 (MJD1) gene product, ataxin-3, which includes an expanded polyQ stretch (79 glutamine repeats, Q79C).^{15,16} As a negative control, ataxin-3 C-terminus with 22 or 35 glutamine repeats (Q22C and Q35C, respectively) was used.^{15,16} BIP readily suppressed Q79C-induced cell death in a neuroblastoma cell line (Neuro-2a) (Figure 1a and b) and in a human embryonic kidney cell line (HEK293T) (Figure 2a). Although these cell lines incorporated BIP very efficiently,⁹ the primary cultured rat cortical neurons showed very low uptake of BIP. To study whether BIP can suppress polyQ-induced cell death in primary cortical neurons, we utilized the protein transduction domain of the human immunodeficiency virus (HIV) trans-activator (TAT)¹⁷ to enhance cell permeability of BIP. PolyQ was expressed by an adenovirus vector.¹⁶ We confirmed that TAT-BIP efficiently entered primary cortical neurons (Supplementary Figure 1), and it inhibited polyQ-induced cell death in these cells (Figure 1c). To confirm the role of Bax in polyQ-induced cell death, we employed small interference RNA (siRNA) targeting Bax mRNA (Figure 1d).

¹Department of Neurology and Neurological Science, Tokyo Medical and Dental University, Tokyo, Japan; ²Departments of Medicine and Pharmacology, Case Western Reserve University, Cleveland, OH, USA; ³Faculty of Life Sciences, Bar-Ilan University, Ramat-Gan, Israel and ⁴Paul F. Glenn Laboratories for the Molecular Biology of Aging, Department of Pathology, Harvard Medical School, Boston, MA, USA

*Corresponding authors: T Yokota, Department of Neurology and Neurological Science, Tokyo Medical and Dental University, Tokyo 113-8519, Japan.

Tel: +81 3 5803 5234; Fax: +81 3 5803 0169; E-mail: tak-yokota.nuro@tmd.ac.jp or S Matsuyama, Departments of Medicine and Pharmacology, Case Western Reserve University, Cleveland, OH 44106, USA. Tel: 216 368 5832; Fax: 216 368 8919; E-mail: shigemi.matsuyama@case.edu

⁵These authors contributed equally to this work

Keywords: polyglutamine; Bax; Ku70; Acetylation; SIRT1

Abbreviations: polyQ, polyglutamine; MJD, Machado–Joseph disease; BIP, Bax-inhibiting peptide; LDH, lactate dehydrogenase; siRNA, small interference RNA; CBP, cyclic-AMP response element-binding protein; HDAC, histone deacetylase; TSA, trichostatin A

Received 22.12.06; revised 23.7.07; accepted 23.7.07; Edited by M Deshmukh; published online 21.9.07

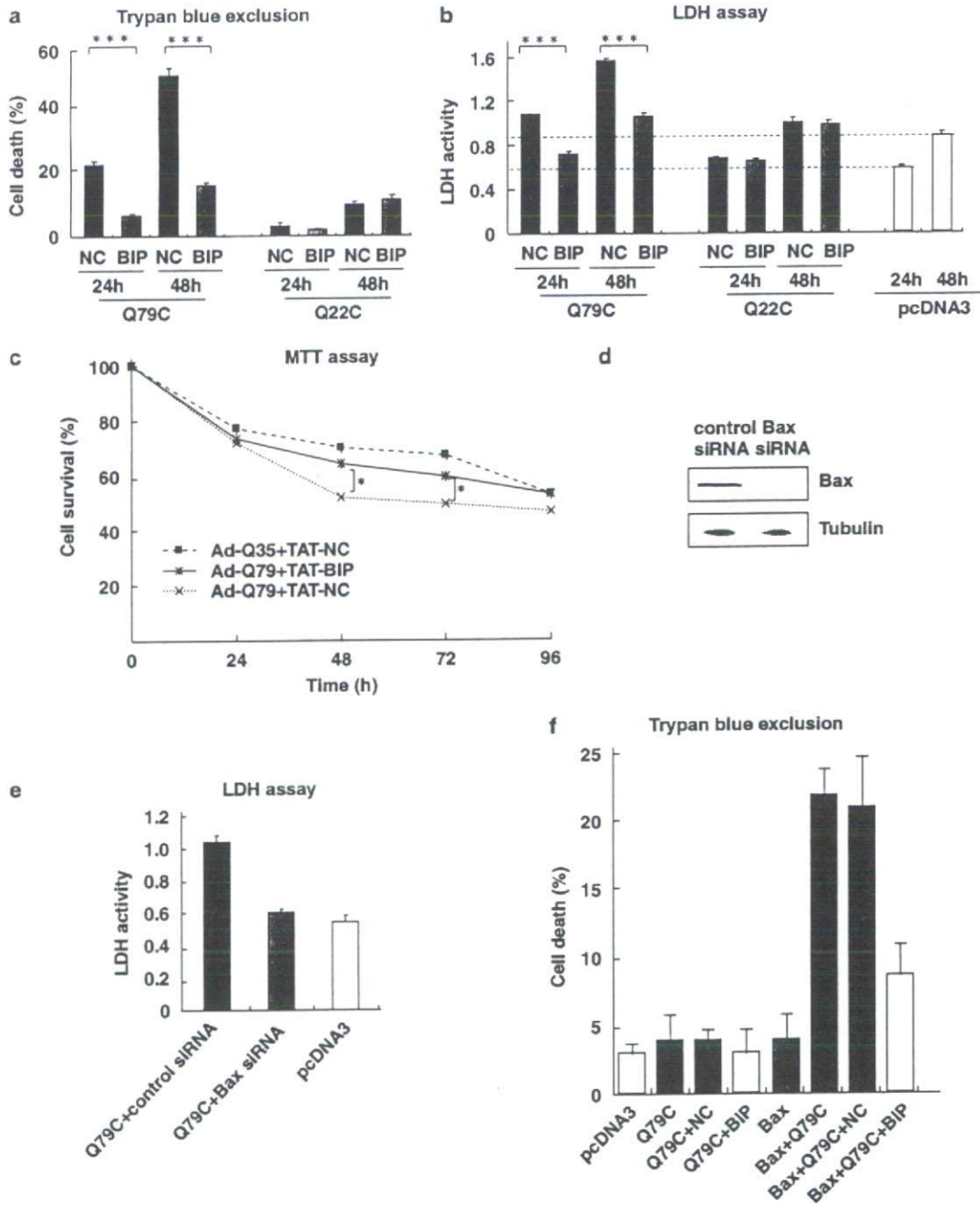


Figure 1 BIP suppresses Q79C-induced cell death. (a and b) Neuro-2a cells in 24-well plates were transfected with pCMX HA-Q22C (0.5 μ g), pCMX HA-Q79C (0.5 μ g) or pcDNA3 (0.5 μ g) in the presence of 200 μ M VPPLK (BIP) or negative control peptide (IPMIK; NC). Cell death was analyzed by Trypan blue exclusion (a) or LDH release into the medium (b) at both 24 and 48 h after transfection; *** P < 0.001. (c) Primary cortical neurons in 24-well plates were infected with Ad-Q79C or Ad-Q35C at m.o.i. 100 in the presence of 80 μ M TAT-VPPLK (TAT-BIP) or negative control peptide (TAT-IPMIK; TAT-NC). Cell death was analyzed by MTT assay at 24, 48, 72 and 96 h after treatment. The relative number of surviving cells was determined in triplicate by estimating the value of unstimulated or uninfected cells as 100%; * P < 0.05. (d and e) The Bax siRNA suppresses Q79C toxicity. HEK293T cells in 24-well plates were transfected with pCMX HA-Q79C (0.5 μ g) and 100 nM of control siRNA or Bax siRNA. The suppression of endogenous Bax expression by Bax siRNA was confirmed by Western blotting (d). The effect of Bax siRNA on Q79C-induced cell death is shown (e). (f) DU145 cells (Bax-deficient cells) in six-well plates were transfected with pcDNA3 (1 μ g), pCMX HA-Q79C (1 μ g) or pcDNA3-Bax (0.25 μ g), and were cultured in the presence or absence of 200 μ M VPMLK (BIP) or negative control peptide (IPMIK; NC). Cell death was analyzed by Trypan blue exclusion at 48 h after transfection

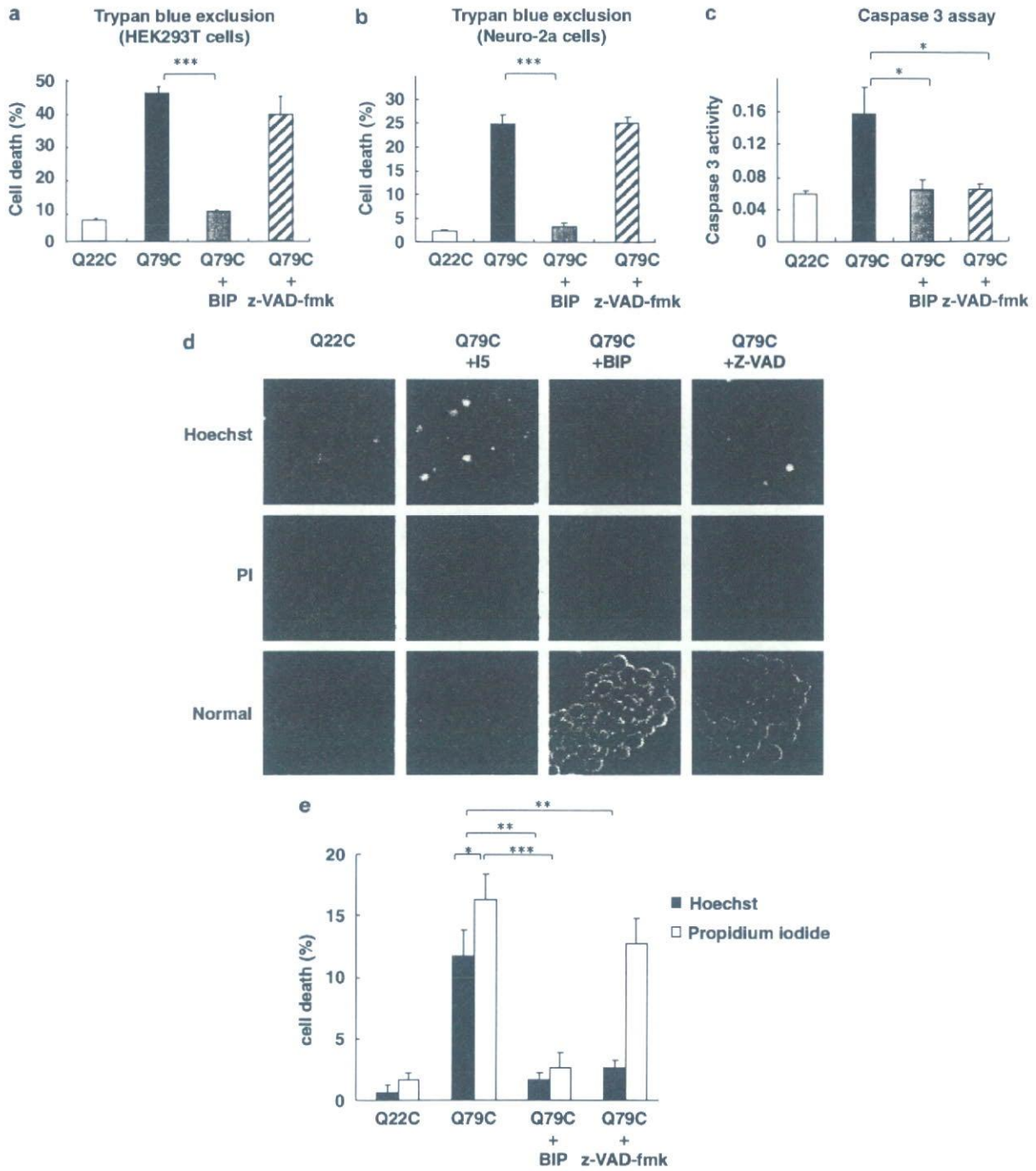


Figure 2 BIP suppresses both caspase-dependent and -independent cell death induced by Q79C. (a–c) HEK293T (a) or Neuro-2a cells (b and c) in 24-well plates were transfected with pCMX HA-Q22C (0.5 μ g) or pCMX HA-Q79C (0.5 μ g) in the presence of 200 μ M VPMLK (BIP) or 100 μ M of caspase inhibitor (z-VAD-fmk). At 48 h after transfection, cell death was determined by Trypan blue exclusion (a and b), and apoptotic events were evaluated by caspase 3 activity (c) * P < 0.05 or *** P < 0.001. (d and e) Neuro-2a cells in 24-well plates were transfected with pCMX HA-Q22C (0.5 μ g) or pCMX HA-Q79C (0.5 μ g) in the presence of 200 μ M VPMLK (BIP) or 100 μ M of caspase inhibitor (z-VAD-fmk). At 48 h after transfection, cell death was determined by double staining with Hoechst (d, upper panel), PI (d, middle panel) and normal light field image (d, lower panel). The percentages of apoptotic cells with nuclear condensation and fragmentation and dead cells detected by PI staining (membrane integrity loss) are presented. Results are shown as mean \pm S.E. of triplicated samples

The siRNA significantly inhibited Q79C-induced cell death (Figure 1e). Furthermore, we examined the cytotoxicity of polyQ in a Bax-deficient cell line, DU145 (human prostate cancer cell line).¹⁸ Q79C did not show significant toxicity in DU145 cells, although Q79C induced cell death if Bax expression was restored (Figure 1f). These results suggest that Bax is a key mediator of Q79C-induced cell death.

BIP suppresses Q79C-induced nuclear fragmentation and cytoplasmic vacuolation. Next, we examined the effect of a pan-caspase inhibitor on Q79C-induced cell death, because Bax activates the caspases resulting in apoptosis.⁶ Unexpectedly, the pan-caspase inhibitor, z-VAD-fmk, did not show a significant cytoprotective effect against Q79C toxicity when cellular viability was examined by Trypan blue exclusion (Figure 2a and b) and lactate dehydrogenase (LDH) release from the cells into the medium (data not shown). To further determine the role of caspase in Q79C-induced cell death, we examined the increase in caspase activity and the occurrence of nuclear fragmentation. We found that Q79C induced caspase activation (Figure 2c) and nuclear fragmentation (Figure 2d and e), both of which could be attenuated by both inhibitors of Bax (BIP) and of caspases (z-VAD-fmk). Of note, the number of apoptotic cells detected by the presence of nuclear fragmentation (Figure 2d and e) was less than the net number of dead cells detected by staining of Trypan blue (Figure 2b) and propidium iodide (PI) (Figure 2d and e), suggesting that Q79C activates both caspase-dependent and -independent cell death pathways.

PolyQ-induced cell death is associated with an increased number of enlarged vacuoles.^{19–21} We also found that Neuro-

2a cells with Q79C expression showed marked cytoplasmic vacuolation. BIP suppressed cytoplasmic vacuolation (Figure 3a and b), whereas the caspase inhibitor did not. These results suggest that Q79C-induced vacuolation is Bax-dependent and caspase-independent. Collectively, BIP suppressed both caspase-dependent nuclear fragmentation and caspase-independent cytoplasmic vacuolation elicited by polyQ.

Q79C expression induces Ku70 acetylation that releases Bax from Ku70. Because BIP is designed from Ku70 which prevents Bax-mediated cell death,^{8–10} we examined whether Q79C had any influence on the binding between Ku70 and Bax. Q79C significantly decreased the interaction between Bax and Ku70 (Figure 4a and b). Furthermore, we found that Q79C induced significant acetylation of Ku70 (Figure 4c). To be noted, the acetylation of Ku70 is known to dissociate Bax and Ku70.¹² Two lysine (K) residues in Ku70, K539 and K542, are critical acetylation sites that influence Ku70-Bax binding.¹² To test whether Ku70 acetylation plays a role for the activation of Bax by polyQ, we generated acetylation-resistant mutants of Ku70 by substituting K539 and K542 with arginine (R) or glutamine (Q), respectively. Acetylation-resistant Ku70 mutants (K539R and K542R)¹² suppressed Q79C-induced cell death more efficiently than wild-type Ku70 (Figure 4d). In contrast, the acetylation-mimicking Ku70 mutants (K539Q and K542Q),¹² could not suppress Q79C-induced cell death. The expression of these Ku70 mutants alone did not affect the cell viability. These results support the hypothesis that Q79C expression activates Bax, at least in part, through Ku70 acetylation.

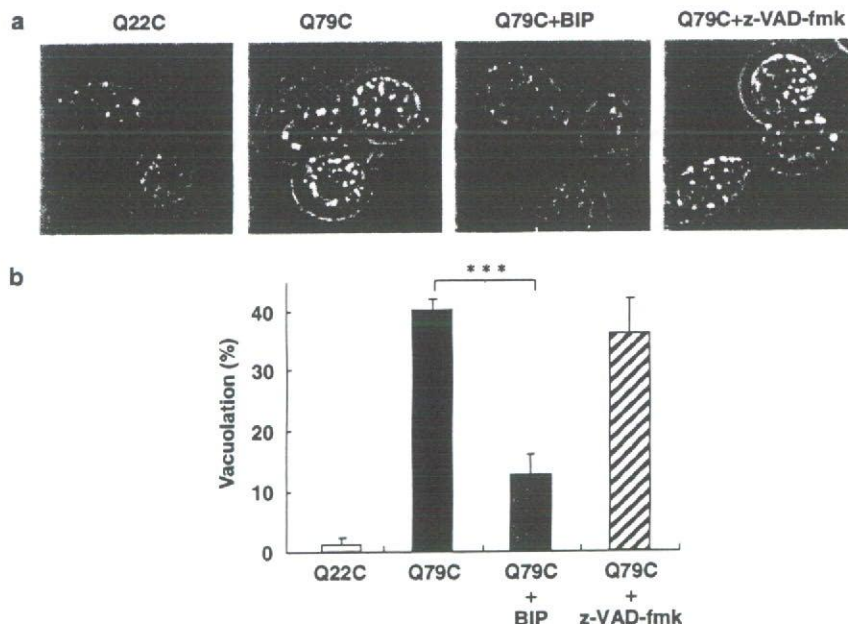


Figure 3 BIP suppresses Q79C-induced cytoplasmic vacuolation. Neuro-2a cells were transfected with pCMX HA-Q22C (0.5 μ g) or pCMX HA-Q79C (0.5 μ g) in the presence of 200 μ M VPPLK (BIP) or 100 μ M z-VAD-fmk. (a) At 48 h after transfection, the percent of cells with cytoplasmic vacuolation to all living cells were evaluated under optical microscopy ($\times 400$); (b) $***P < 0.001$

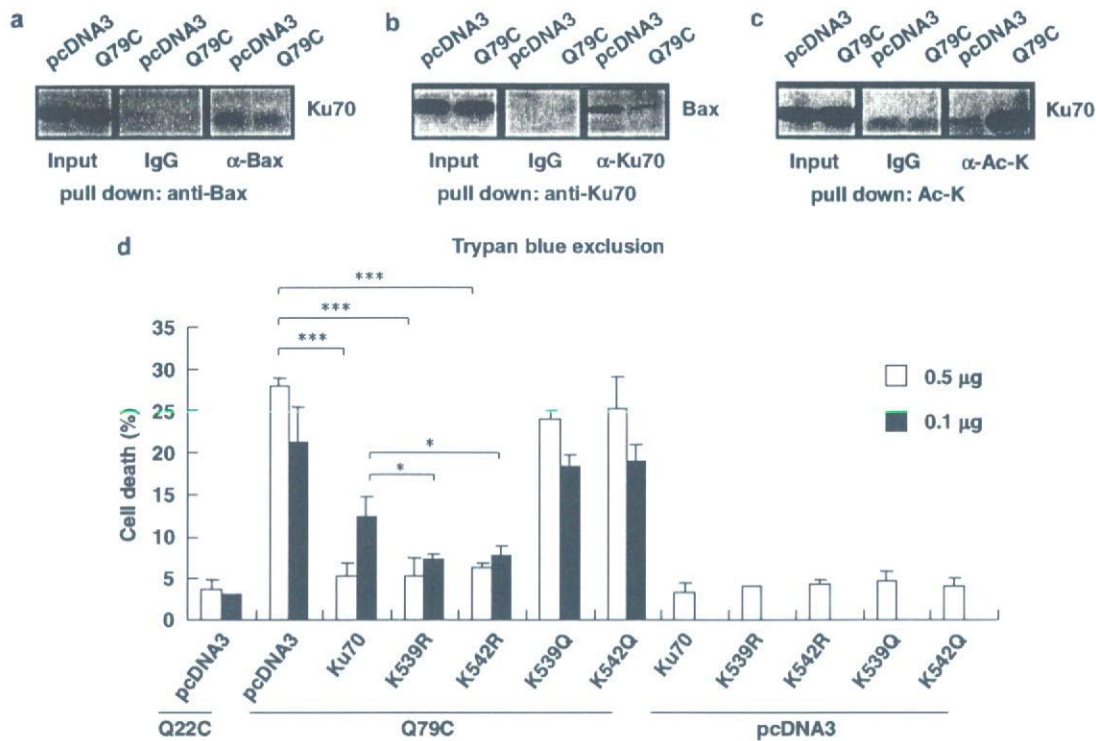


Figure 4 Q79C expression induces Ku70 acetylation that releases Bax from Ku70. (a and b) HEK293T cells in 10-cm dishes were transfected with pcDNA3 (10 μ g) or pCMX HA-Q79C (10 μ g). At 48 h after transfection, cells were harvested and immunoprecipitation was performed using anti-Bax (a) and anti-Ku70 monoclonal antibodies (b). Normal mouse IgG (IgG) was used as a negative control. Western blotting was performed with anti-Ku70 (a) or anti-Bax polyclonal (b) antibody. (c) HEK293T cells in 10-cm dishes were transfected with pcDNA3 (10 μ g) or pCMX HA-Q79C (10 μ g). After 48 h, cells were harvested and immunoprecipitation was performed using anti-pan-acetylated lysine monoclonal antibody, and the acetylated Ku70 was detected by Western blotting with anti-Ku70 polyclonal antibody. (d) Neuro-2a cells in 24-well plates were co-transfected with pCMX HA-Q79C/Q22C (0.5 μ g) and pcDNA3 (0.1 μ g or 0.5 μ g), wild-type Ku70 (0.1 μ g or 0.5 μ g) or Ku70 mutants (0.1 μ g or 0.5 μ g) bearing K \rightarrow R (acetylation-resistant mutation) or K \rightarrow Q substitutions (mutation that mimics acetylation) at positions K539 and K542. Cell death was analyzed by Trypan blue exclusion (d) at 48 h after transfection; *** $P < 0.001$ or * $P < 0.05$

Ku70 and BIP inhibit Bax conformational change induced by polyQ expression. In cells with apoptotic stimuli, Bax is known to change its conformation, and the conformational change can be detected using the 6A7 anti-Bax monoclonal antibody that recognizes the N-terminus of Bax by immunoprecipitation.^{22,23} The N-terminus exposure is an early step of Bax activation that occurs in the cytosol, and this conformational change is considered a prerequisite for membrane insertion of Bax at mitochondria and multimerization of Bax.^{22–24} We found that Ku70 wild type and acetylation-resistant Ku70 (Ku70(K539R)), but not acetylation-mimicking Ku70 mutant (Ku70(K539Q)), inhibited the conformational change that was induced by polyQ expression (Figure 5a and b). It was also confirmed that BIP treatment significantly blocked Bax conformational change (Figure 5c). These results further support our hypothesis that Ku70 as well as BIP protect cells from polyQ toxicity by inhibiting Bax-mediated cell death.

Q79C binds Ku70 and histone acetyl transferase. Next, we examined how Q79C expression results in the acetylation of Ku70. The cyclic-AMP response element-binding protein (CBP) has been shown to acetylate cytosolic Ku70 in response to apoptotic stimuli.¹² Q79C is known to bind

CBP in the nucleus.⁴ We found that this interaction occurs in the cytosol too. We performed co-immunoprecipitation of polyQ and CBP using the cytosolic fraction and found that CBP was co-immunoprecipitated with Q79C, but not with Q22C (Figure 6a). In addition, we found that Ku70 binds both Q79C and Q22C in the cytosolic fraction (Figure 6b). We further confirmed the interaction of Q79C and CBP in the cytosol fraction (Figure 6c). These results suggest that Q79C stimulates Ku70 acetylation by bridging Ku70 and CBP (Figure 6d).

SIRT1 deacetylase and resveratrol rescue Q79C-induced cell death. The significant role of Ku70 acetylation in Q79C-induced cell death implies the possibility that the stimulation of deacetylases could reduce the polyQ toxicity. First, we examined the effect of the SIRT1 deacetylase, which has been demonstrated to deacetylate Ku70.¹² Overexpression of SIRT1 suppressed Q79C-induced cell death in Neuro-2a cells (Figure 7a and b). Small polyphenolic molecules such as resveratrol have been found to increase the affinity of SIRT1 and its target proteins.²⁵ We found that resveratrol markedly suppressed the cell death induced by Q79C in the HEK293T cells and primary cortical neurons (Figure 7c–e). We confirmed that SIRT1 expression and resveratrol

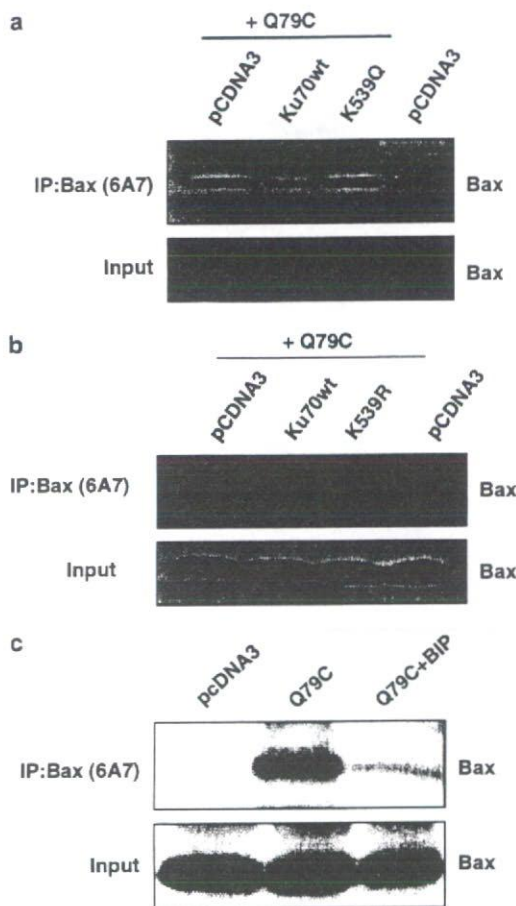


Figure 5 Ku70 and BIP inhibit Bax conformational change induced by polyQ expression. (a and b) Ku70 inhibits conformational change of Bax induced by Q79C. Neuro2a cells in 10-cm dishes were transfected with pcDNA3 (5 μ g) or pCMX HA-Q79C (5 μ g) together with pCMV-2B-Ku70 (5 μ g), K539Q (acetylation-mimicking mutant) (5 μ g) or K539R (acetylation-resistant mutant). After 48 h, cells were harvested and immunoprecipitation was performed using 6A7 anti-Bax monoclonal antibody. (c) HEK293T cells in 10-cm dishes were transfected with pcDNA3 (10 μ g) or pCMX HA-Q79C (10 μ g) in the presence or absence of 200 μ M VPMLK (BIP). After 48 h, cells were harvested and immunoprecipitation was performed using 6A7 anti-Bax monoclonal antibody

treatment reduced the acetylation levels of Ku70 that was increased by Q79C expression (Figure 7f).

Discussion

We demonstrated that the inhibition of Bax by Ku70 and BIP markedly protected cells from polyQ toxicity. These results indicate that Bax plays a key role in polyQ toxicity. Our data also suggest that polyQ expression activates two different pathways of cell death. One is caspase-dependent cell death associated with nuclear fragmentation, and the other is caspase-independent cell death associated with cytoplasmic vacuolation, both of which were dramatically decreased by BIP. Cytoplasmic vacuolation has been observed in the neurons of patients with polyQ diseases.^{19–21} Importantly, Bax is known to induce both caspase-independent and -dependent cell death with cytoplasmic vacuolation when

caspase activity is inhibited or absent.^{26–28} These previous reports support our hypothesis that Bax is a key mediator of Q79C-induced cell death associated with cytoplasmic vacuolation. Recently, an elevated expression of Bax was reported in the brain of polyQ-transgenic mouse.^{29,30} We also observed that the number of pontine nucleus and microglia stained by anti-Bax 6A7-Ab in the brain section of MJD patient was significantly higher than those of normal controls (Supplementary Figure 3). Although this result is consistent with our findings in cell culture system, there are potential limitations of such experiments using human tissue, as the conditions and timing of specimen collection cannot be strictly controlled. Further extensive investigation is needed to determine the role of Bax in MJD pathogenesis in patient brain.

The significant ability of BIP to suppress Q79C-induced cell death suggests the possibility that Q79C expression causes dissociation of Ku70 from Bax. Previously, we reported that apoptotic stimuli decreased cytosolic levels of Ku70, and that this change may be one of the mechanisms for Ku70 dissociation from Bax.³¹ However, in the case of Q79C expression, the decrease of Ku70 levels was not clear (Figure 4a and c, Ku70 input). The acetylation of Ku70 is known to be another mechanism releasing Bax from Ku70.¹² As shown in Figure 4, Q79C induced a significant acetylation of Ku70. We also confirmed that Ku70 mutants mimicking acetylation did not suppress Q79C-induced cell death, whereas acetylation-resistant Ku70 mutants rescued cells from Q79C toxicity more efficiently than Ku70 wild type. These results suggest that Ku70 acetylation is one of the major causes of Bax activation in Q79C-expressing cells.

SIRT1, one of the mammalian silent information regulator 2 (Sir2) homologues, was identified as a cell survival factor that protects cells from DNA damage.³² SIRT1 was shown to have the activity to deacetylate several transcription factors, and through this activity, SIRT1 regulates a wide array of cellular processes for cell defense and survival under various stress conditions (reviewed by Baur and Sinclair²⁵). Recently, resveratrol, an activator of the Sir2 histone deacetylase (HDAC),²⁵ has been reported to rescue polyQ-induced neuronal dysfunction in *Caenorhabditis elegans*.³³ Similarly, in the present study, SIRT1 deacetylase and resveratrol both effectively rescued cultured cells from polyQ toxicity. We confirmed that Ku70 was acetylated by Q79C and that Ku70 was deacetylated by resveratrol and SIRT1. These observations support our hypothesis that Ku70 acetylation plays an important role in Q79C-induced cell death.

It has been hypothesized that polyQ toxicity is caused by decreased histone acetylation, as polyQ sequesters histone acetyl transferase (HAT) (e.g. CBP) from chromosomes.^{2,3} The subsequent suppression of histone acetylation decreases cellular transcriptional activities, and these changes are implicated to cause polyQ toxicity. Based on this hypothesis, the maintenance of histone acetylation by HDAC inhibitors, such as trichostatin A (TSA), has been examined for the reduction of polyQ toxicity.^{3,34,35} However, an HDAC inhibitor was recently shown to induce apoptosis in neuroblastoma cells by increasing Ku70 acetylation and promoting Bax-mediated cell death.¹⁴ Therefore, it is plausible that HDAC inhibitors have a 'double-edge' activity in the context of

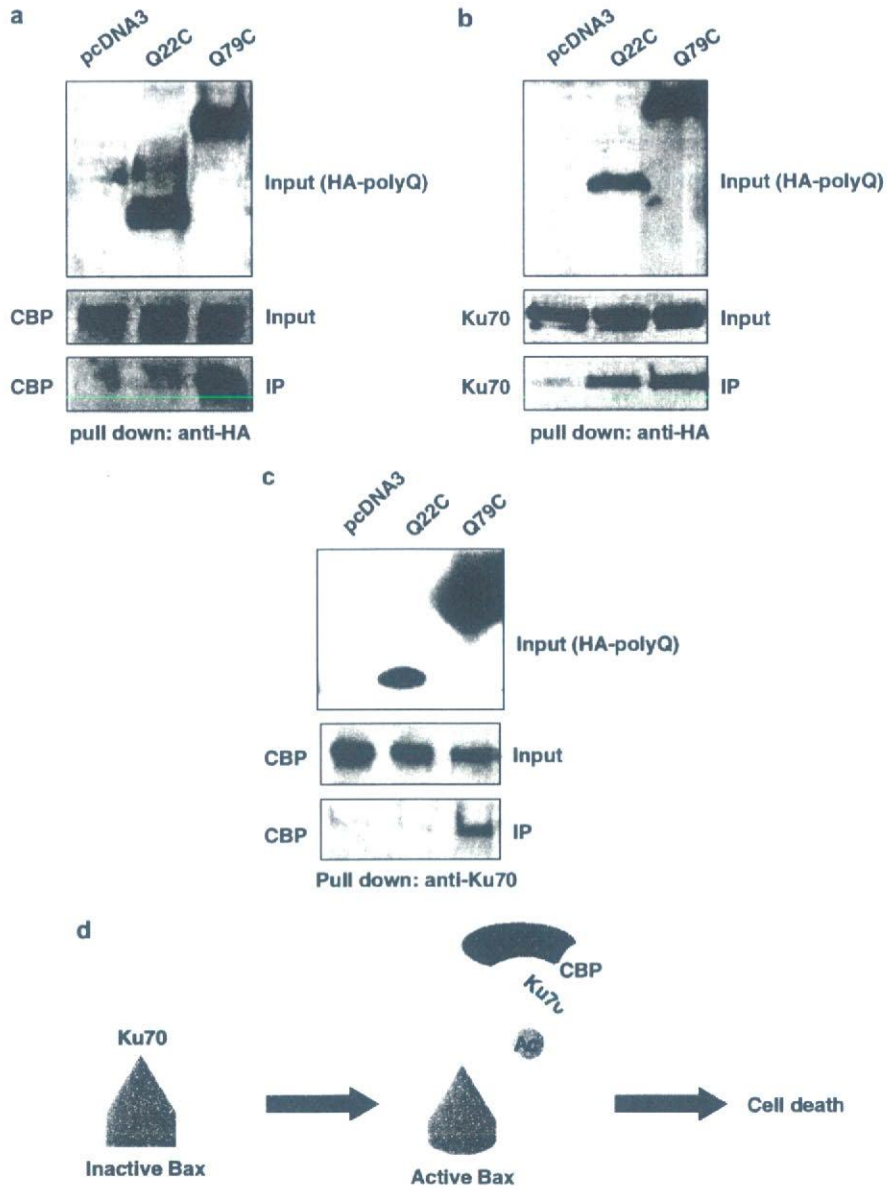


Figure 6 Q79C binds Ku70 and CBP. (a–c) HEK293T cells were transfected as described in Figure 4a and b, and the cytosolic fraction was used for immunoprecipitation. Immunoprecipitation was performed using anti-HA (a and b) or anti-Ku70 monoclonal antibody (c). Western blotting analyses of HA-tagged polyQ (Q22C and Q79C), CBP and Ku70 are shown. (d) Schematic representation of Bax activation by Ku70 acetylation during Q79C-induced cell death

polyQ toxicity; they attenuate polyQ toxicity by maintaining histone acetylation in the nucleus, but promote Bax-mediated cell death by acetylating Ku70 in the cytosol. In cultured cells, TSA can attenuate Q79C-induced cell death only at the lower doses (3–10 nM), whereas it enhances cell death at the higher doses (more than 20 nM) (Supplementary Figure 2). Actually, the therapeutic effect of an HDAC inhibitor was observed only within a narrow range of lower doses, and the effect changed to be toxic at higher doses in polyQ transgenic mice.³⁵ These results suggest that the use of HDAC inhibitors in polyQ diseases requires careful consideration to avoid causing a lethal degree of Ku70 acetylation. The present study focused

on the toxicity of expanded polyQ derived from the causative gene (mutated ataxin3) of MJD. Thus, further study is needed to examine whether our observation can be generally confirmed in other types of toxic polyQ such as that of Huntington's disease and spinocerebellar ataxia type 1 (SCA1).

In conclusion, we propose that Bax is a key mediator of Q79C-induced cell death and that Bax activation is mediated through acetylation of Ku70, which dissociates Bax from Ku70. Our hypothesis is based on the observation in cell culture studies, and further extensive studies using *in vivo* models are clearly needed. The present study suggests that

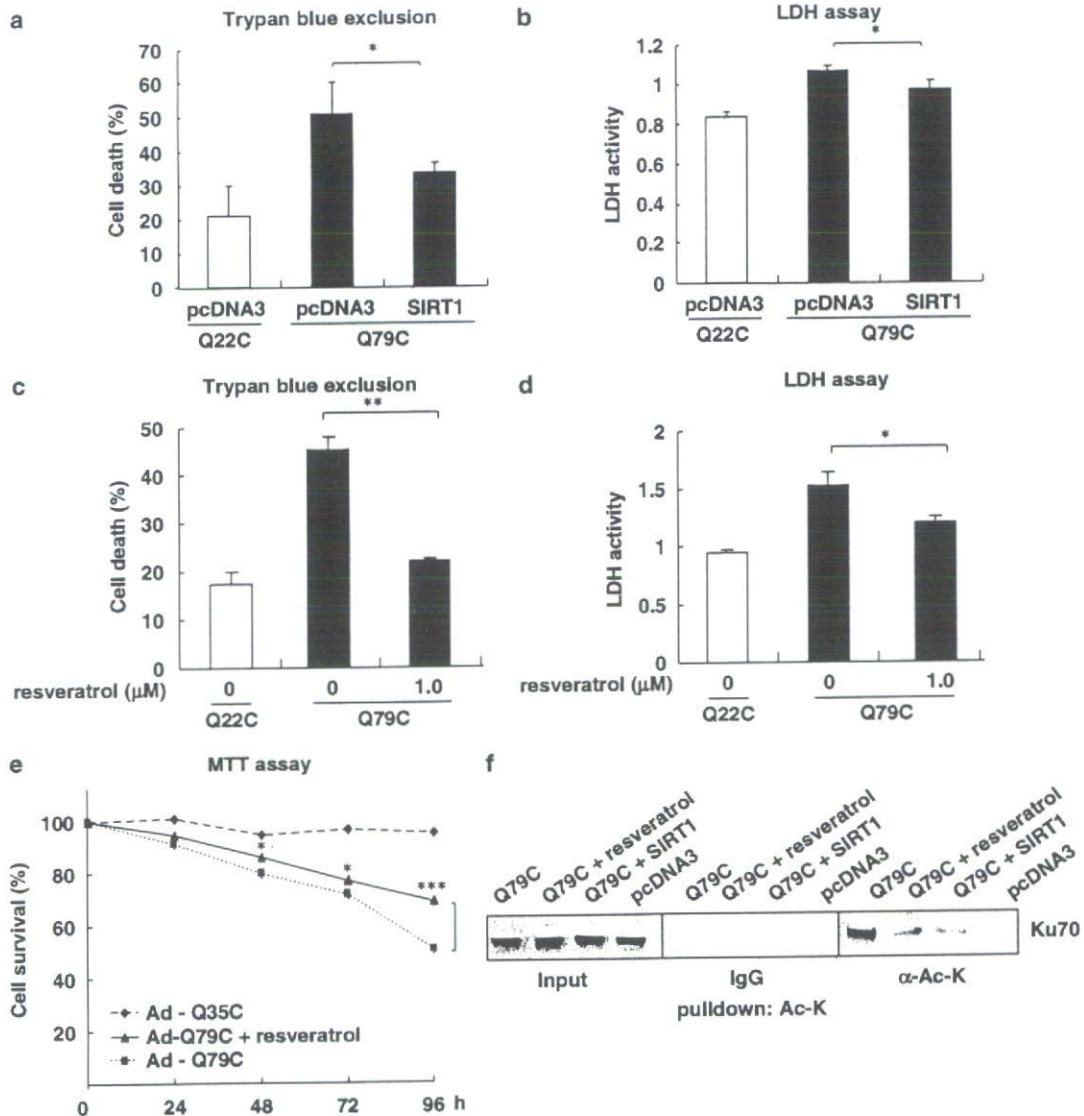


Figure 7 Effects of SIRT1 and resveratrol on Q79C-induced cell death. Neuro-2a cells in 24-well plates were co-transfected with pCMX HA-Q79C or -Q22C (0.5 μg) and pcDNA3 (0.5 μg), or pcDNA3-SIRT1 (0.5 μg). Cell death was analyzed by Trypan blue exclusion (a) or LDH release into the medium (b) at 48 h after transfection; * $P < 0.05$. HEK293T cells in 24-well plates were transfected with pCMX HA-Q79C (0.5 μg) or pCMX HA-Q22C (0.5 μg) in the presence of resveratrol (1 μM). Cell death was assessed by Trypan blue exclusion (c) or LDH release into the medium (d) at 72 h after transfection; ** $P < 0.01$ or * $P < 0.05$. (e) Primary cortical neurons in 24-well plates were infected with Ad-Q79C or Ad-Q35C at m.o.i. 100 in the presence of resveratrol (1 μM). Cell death was analyzed by MTT assay at 24, 48, 72 and 96 h after treatment. The relative number of surviving cells was determined in triplicate by estimating the value of unstimulated or uninfected cells as 100%; *** $P < 0.001$ or * $P < 0.05$. (f) HEK293T cells in 10-cm dishes were transfected with pCMX HA-Q79C (5 μg) and pcDNA3-SIRT1 (5 μg), or with pCMX HA-Q79C (5 μg) in the presence of resveratrol (1 μM). After 48 h, cells were harvested and immunoprecipitation was performed using anti-pan-acetyl-lysine monoclonal antibody. The acetylated Ku70 was detected by Western blotting with anti-Ku70 polyclonal antibody

the inhibition of Bax by BIPs or Ku70 may provide a new strategy to develop therapeutics for MJD.

Materials and Methods

Plasmid constructs and recombinant adenoviruses. The expression plasmids of ataxin-3 were kindly given Dr. Akira Kakizuka. The MJD1 cDNA in the plasmid was a truncated fragment including either 22 (normal, pCMX HA-Q22C) or 79 (expanded, pCMX HA-Q79C) repeats of CAG, and was hemagglutinin (HA)-fused on the N-terminus. The plasmids, pcDNA3-Bax and

pCMV 2B-Flag-Ku70 have been described previously.¹² pCMV 2B-Flag-Ku70 K539R/K542R/K539Q/K542Q were generated by QuickChange Site-Directed Mutagenesis Kit from Stratagene. SIRT1 expression plasmid was generated by subcloning the coding sequence of SIRT1 cDNA (kindly provided by Dr. Shinichirou Imai) into the pcDNA3 vector (Invitrogen). Recombinant adenoviruses encoding Flag-Q79C and Flag-Q35C were constructed as described previously.³⁶

Cell culture and transfection. HEK293T, Neuro-2a and DU145 cells were cultured in DMEM containing 10% fetal bovine serum. Transfection of plasmids was